



Nonparaxial solitons and the dynamics of solitary waves for the coupled nonlinear Helmholtz systems

Yufeng Qian¹ · Jalil Manafian^{2,3} · Mohammed Asiri⁴ · Khaled Hussein Mahmoud⁵ · Ali Ihsan Alanssari⁶ · Abdullah Saad Alsubaie⁵

Received: 18 October 2022 / Accepted: 26 July 2023 / Published online: 20 September 2023
© The Author(s), under exclusive licence to Springer Science+Business Media, LLC, part of Springer Nature 2023

Abstract

In this paper, the nonparaxial solitons in a dimensionless coupled nonlinear Schrödinger system with cross-phase modulation, which enables the propagation of ultra-broad nonparaxial pulses in a birefringent optical waveguide are studied. By noticing that the system is a non-integrable one, and also diverse forms of solitary wave solutions by using the Hirota's bilinear scheme are reached. The binary bell polynomials and bilinear transformation and also the related theorem for getting to the bilinear form of nonlinear system are noticed. In particular, five forms of function solution including soliton, bright soliton, singular soliton, periodic wave and singular form of solutions are investigated. To achieve this, an illustrative example of the coupled nonlinear Helmholtz systems is provided to demonstrate the feasibility and reliability of the procedure is used in this study. The effect of the free parameters on the behavior of acquired figures of a few obtained solutions for two nonlinear rational exact cases was also discussed. We believe that our results would pave a way for future research generating optical memories based on the nonparaxial solitons.

Keywords Nonparaxial solitons · Hirota bilinear technique · Soliton solution · Periodic wave · Coupled nonlinear Helmholtz systems

1 Introduction

In this paper, the generation of non-slowly varying electric fields is concerned in a physical setting of liquid crystals or birefringent optical fibers to the coupled nonlinear Helmholtz systems. The following dimensionless coupled equations can be utilized to specify the propagation of incoherently coupled and orthogonally polarized waveguide modes in a Kerr medium (Tamilselvan et al. 2016) as follows

$$i\Sigma_{l,z} + \Lambda\Sigma_{l,zz} + \frac{\alpha}{2}\Sigma_{l,tt} + \delta(|\Sigma_l|^2 + |\Sigma_{3-l}|^2)\Sigma_l = 0, \quad l = 1, 2, \quad (1.1)$$

where Σ_l , ($l = 1, 2$) symbolize the orthogonally polarized components of the optical modes and the variables z , and t , respectively, represent longitudinal and transverse co-ordinates. The second expression Λ in Eq. (1.1) is the non-paraxial parameter (NP) and correspond

to $1/2k_0L$ (Tamilselvan et al. 2016). The group-velocity dispersion (GVD) is stated by the parameter α and in this study, it is apportioned to be operating in the anomalous dispersion regime. Nonlinearity and its coupling parameters are denoted by using the terms δ and α , respectively, which are attributed by the symmetry properties of third-order susceptibility tensor.

The evolution of broad optical beams in Kerr like nonlinear media can be well stated by the coupled nonlinear Helmholtz (CNLH) type equations. Equation (1.1) has been studied in Christian et al. (2006) and bright and dark soliton solutions have been reported for focusing and defocusing nonlinearities respectively. Collision investigations of solitons in CNLH system revealed the fact that the interaction angle between two solitons is changed by altering the nonparaxial parameter (Chamorro-Posada and McDonald 2006). In Tamilselvan et al. (2016), the authors obtained a class of elliptic wave solutions of CNLH equations describing nonparaxial ultra-broad beam propagation in nonlinear Kerr-like media, in terms of the Jacobi elliptic functions and also discussed their limiting forms. Song et al. (2020) discussed a quartic eigenvalue problem of CNLH system arising in the context of an optical waveguiding problem involving atomically thick 2D materials. Also, the exact solutions of CNHE equations via the $\exp(-\Phi(\epsilon))$ expansion method have been obtained (Singh et al. 2020).

Due to the unique physical properties of interaction between multiple coherent optical fields, a number of practical applications in optical transmission systems have been put forward such as switching, and modulators (Kivshar and Agrawal 2003). Also, the dynamics of optical modes traversing by way of the birefringent fiber can be mathematically governed by a system of coupled nonlinear Schrödinger equations, which results in a shape-preserving solution due to their multiple component natures. The vector soliton is produced when the nonlinearity of the fiber causes coupling between diverse optical modes during the propagation in the multimode optical fiber, which vector soliton provides an efficient way to a variety of practical applications such as channel wavelength division-multiplexing, pulse generation, and high-speed optical switching (Hansryd et al. 2002). Soliton interactions can be divided into two types: coherent interactions and incoherent interactions (Ku et al. 2005).

In the last decades, researchers have developed numerous methods such as, the generalized rational $\tan(\phi/2)$ -expansion technique (Liu et al. 2023), k -lump and k -kink solutions (Gu et al. 2022), the extended sinh-Gordon equation expansion method (Ali et al. 2023), the multiple Exp-function method (Liu et al. 2018), the seismic wave attenuation (Bouchaala et al. 2022), the compressional seismic wave attenuation (Bouchaala et al. 2019), the Hirota's bilinear method (Manafian and Lakestani 2020), the stress and dynamic analysis of truck ladder chassis (Mahmoodi-k et al. 2014), dual unscented kalman filter algorithm method (Davoodabadi et al. 2014), the quantum-mechanical method (Della Volpe and Siboni 2022), multiple soliton solutions and fusion interaction phenomena (Wen and Xu 2013), the truncated Painlevé series (Ren et al. 2019), single-lap adhesive joints method (Ghasemvand et al. 2023), truss optimization with metaheuristic algorithms method (Aslanova 2020), the modified Pfaffian technique (Liu et al. 2021), linear spectral dynamic analysis method (Madina and Gumilyov 2020), a carver matrix and providing solutions (Zahedi and Golivari 2022), a random decrement signature and artificial neural network algorithm techniques (Mojtahedi et al. 2022), logistic damping effect in chemotaxis models (Lyu and Wang 2023), the one-dimensional attraction-repulsion Keller–Segel model (Jin and Wang 2015), fracture analysis of fluid-structure interactions (Dai et al. 2023), energy relaxation of hot electrons (Du et al. 2023), variable weighted iterative learning (Xu et al. 2023), the dynamics analysis

of Gompertz virus disease model (Wang et al. 2023), a novel data generation and quantitative characterization method (Sun et al. 2023), nonlinear energy recharging and consumption (Xiao et al. 2021), the renewable energy sources (Jiang et al. 2022), a hybrid convolutional neural network (Erfeng and Ghadimi 2022; Han and Ghadimi 2022), a hybrid robust-stochastic approach (Cai et al. 2019; Yu et al. 2020), a optimal chiller loading (Saedi et al. 2019), the distributed series reactor (Yuan et al. 2020), an intelligent algorithm (Mir et al. 2020), the deep learning method (Zhang et al. 2022), the power systems (Chen et al. 2022), dual-form of generalized nonlocal nonlinearity (Li et al. 2023), high-order uncertain nonlinear systems (Guo and Hu 2023; Meng et al. 2023; Guo et al. 2023, 2023), nonlinear networked control systems (Zhong et al. 2022), and so forth (Bai et al. 2022; Xiang et al. 2023; Moghadam and Ebrahimi 2021; Brown and Mazumder 2021).

In the context of water wave theory, the complete study on the related physical systems were executed by exploring several integrable as well as non-integrable evolution equations in one and higher dimensions (Lakshmanan and Rajasekar 2003). Integrability is a fascinating property to characterize any dynamical models in addition to existence of Lax pair and infinitely many conserved quantities. The ancillary techniques containing direct algebraic techniques, auxiliary equation method, Kudryashov expansion method, Riccati-Bernoulli sub-ODE method, sinh-Gordon expansion method, cosh-tanh method, simplest equation method, and so on are utilized widely to get different classes of travelling wave solutions (Wazwaz 2009). Especially, these methodologies provide a variety of exotic wave patterns, including solitons, breathers, lumps, dromions, rogue waves, and elliptic waves. On the advantageous part, the Hirota bilinear method is an intermediate tool which can be utilized to extract the localized nonlinear wave solution to most of the integrable as well as a few class of non-integrable soliton models and it becomes a widely used tool to obtain several localized nonlinear wave solutions (Zhou et al. 2021; Manafian et al. 2020; Alimirzalu et al. 2021; Pourghanbar et al. 2020; Dawod et al. 2023; Mehrpooya et al. 2021).

The general form of the fractional reduced differential transform method to (N+1)-dimensional fractional order partial differential equations were studied (Arshad et al. 2017). The unstable non-linear Schrödinger dynamical models has been investigated analytically by utilizing the tow variable (G'/G)-expansion approach (Shehzad et al. 2023). The weakly nonlinear wave propagation theory in the occurrence of magnetic fields in fluids of superposed was studied. Also, soliton and other kinds solutions of (2+1)-dimensional elliptic nonlinear Schrödinger equation were constructed (Seadawy et al. 2020).

In this paper, some solutions including soliton, bright soliton, singular soliton, periodic wave and singular form of solutions by Hirota bilinear method are also obtained.

Inspired by the previous work, the aim of the paper is to investigate the nonparaxial solitons and other form of solutions. The outline of the paper is as follows. In Sect. 2, the bilinear equations through Hirota operator for the CNLH system are obtained. Furthermore, in Sect. 3, different forms of solitary wave solutions are established. Finally, the conclusions are provided in Sect. 3.5.3.

2 Binary Bell polynomials and bilinear transformation

By way of Ma (2013) and $A = A(x_1, x_2, \dots, x_n)$ we have

$$\begin{aligned}
 B_{n_1, x_1, \dots, n_j, x_j}(A) &\equiv B_{n_1, \dots, n_j}(A_{d_1, x_1, \dots, d_j, x_j}) \\
 &= e^{-A} \partial_{x_1}^{n_1} \dots \partial_{x_j}^{n_j} e^A,
 \end{aligned}
 \tag{2.1}$$

with the multi-D Bell polynomials as

$$\begin{aligned}
 A_{d_1, x_1, \dots, d_j, x_j} &= \partial_{x_1}^{d_1} \dots \partial_{x_j}^{d_j} A, \quad A_{0, x_i} \\
 &\equiv A, \quad d_1 = 0, \dots, n_1; \dots; d_j = 0, \dots, n_j,
 \end{aligned}$$

and we get

$$\begin{aligned}
 B_1(A) &= A_x, \quad B_2(A) = A_{2x} + A_x^2, \quad B_3(A) = A_{3x} + 3A_x A_{2x} + A_x^3, \dots, \quad A = A(x, t), \\
 B_{x,t}(A) &= A_{x,t} + A_x A_t, \quad B_{2x,t}(A) = A_{2x,t} + A_{2x} A_t + 2A_{x,t} A_x + A_x^2 A_t, \dots
 \end{aligned}
 \tag{2.2}$$

The multi-dimensional binary Bell polynomials can be stated as

$$C_{n_1, x_1, \dots, n_j, x_j}(\mu_1, \mu_2) = B_{n_1, \dots, n_j}(A) \Big|_{A_{d_1, x_1, \dots, d_j, x_j} = \begin{cases} \mu_{1, d_1, x_1, \dots, d_j, x_j}, & d_1 + d_2 + \dots + d_j, \text{ is odd} \\ \mu_{2, d_1, x_1, \dots, d_j, x_j}, & d_1 + d_2 + \dots + d_j, \text{ is even.} \end{cases}}
 \tag{2.3}$$

The following properties are as

$$C_x(\mu_1) = \mu_{1,x}, \quad C_{2x}(\mu_1, \mu_2) = \mu_{2,2x} + \mu_{1,x}^2, \quad C_{x,t}(\mu_1, \mu_2) = \mu_{2,x,t} + \mu_{1,x} \mu_{1,t}, \dots
 \tag{2.4}$$

Proposition 2.1 Let $\mu_1 = \ln(\Omega_1/\Omega_2)$, $\mu_2 = \ln(\Omega_1\Omega_2)$, then the relations between binary Bell polynomials and Hirota D-operator reads

$$C_{n_1, x_1, \dots, n_j, x_j}(\mu_1, \mu_2) \Big|_{\mu_1 = \ln(\Omega_1/\Omega_2), \mu_2 = \ln(\Omega_1\Omega_2)} = (\Omega_1\Omega_2)^{-1} D_{x_1}^{n_1} \dots D_{x_j}^{n_j} \Omega_1\Omega_2,
 \tag{2.5}$$

with Hirota operator

$$\prod_{i=1}^j D_{x_i}^{n_i} g \cdot \eta = \prod_{i=1}^j \left(\frac{\partial}{\partial x_i} - \frac{\partial}{\partial x'_i} \right)^{n_i} \Omega_1(x_1, \dots, x_j) \Omega_2(x'_1, \dots, x'_j) \Big|_{x_1 = x'_1, \dots, x_j = x'_j}.
 \tag{2.6}$$

Proposition 2.2 Take $\Xi(\gamma) = \sum_i \delta_i \mathfrak{P}_{d_1, x_1, \dots, d_j, x_j} = 0$ and $\mu_1 = \ln(\Omega_1/\Omega_2)$, $\mu_1 = \ln(\Omega_1\Omega_2)$, we have

$$\begin{cases} \sum_i \delta_{1i} B_{n_1, x_1, \dots, n_j, x_j}(\mu_1, \mu_2) = 0, \\ \sum_i \delta_{1i} B_{d_1, x_1, \dots, d_j, x_j}(\mu_1, \mu_2) = 0, \end{cases}
 \tag{2.7}$$

which need to satisfy

$$\mathfrak{R}(\gamma', \gamma) = \mathfrak{R}(\gamma') - \mathfrak{R}(\gamma) = \mathfrak{R}(\mu_2 + \mu_1) - \mathfrak{R}(\mu_2 - \mu_1) = 0.
 \tag{2.8}$$

The generalized Bell polynomials $Y_{n_1, x_1, \dots, n_j, x_j}(\xi)$ is as

$$(\Omega_1 \Omega_2)^{-1} D_{x_1}^{n_1} \dots D_{x_j}^{n_j} \Omega_1 \Omega_2 = C_{n_1, x_1, \dots, n_j, x_j}(\mu_1, \mu_2) \Big|_{\mu_1 = \ln(\Omega_1 / \Omega_2), \mu_2 = \ln(\Omega_1 \Omega_2)} \tag{2.9}$$

$$= C_{n_1, x_1, \dots, n_j, x_j}(\mu_1, \mu_1 + \gamma) \Big|_{\mu_1 = \ln(\Omega_1 / \Omega_2), \gamma = \ln(\Omega_1 \Omega_2)}$$

$$= \sum_{k_1}^{n_1} \dots \sum_{k_j}^{n_j} \prod_{i=1}^j \binom{n_i}{k_i} \mathfrak{P}_{k_1, x_1, \dots, k_j, x_j}(\gamma) B_{(n_1 - k_1)x_1, \dots, (n_j - k_j)x_j}(\mu_1). \tag{2.10}$$

The Cole–Hopf relation is as follows

$$B_{k_1, x_1, \dots, k_j, x_j}(\mu_1 = \ln(\varphi)) = \frac{\varphi_{n_1, x_1, \dots, n_j, x_j}}{\varphi}, \tag{2.11}$$

$$(\Omega_1 \Omega_2)^{-1} D_{x_1}^{n_1} \dots D_{x_j}^{n_j} \Omega_1 \Omega_2 \Big|_{\Omega_2 = \exp(\gamma/2), \Omega_1 / \Omega_2 = \varphi}$$

$$= \varphi^{-1} \sum_{k_1}^{n_1} \dots \sum_{k_j}^{n_j} \prod_{l=1}^j \binom{n_l}{k_l} \mathfrak{P}_{k_1, x_1, \dots, k_l, x_l}(\gamma) \varphi_{(n_1 - k_1)x_1, \dots, (n_l - k_l)x_l}, \tag{2.12}$$

with

$$B_l(\mu_1) = \frac{\varphi_l}{\varphi}, \quad B_{2x}(\mu_1, \beta) = \gamma_{2x} + \frac{\varphi_{2x}}{\varphi}, \quad B_{2x,y}(\mu_1, \mu_2) = \frac{\gamma_{2x} \varphi_y}{\varphi} + \frac{2\gamma_{x,y} \varphi_x}{\varphi} + \frac{\varphi_{2x,y}}{\varphi}. \tag{2.13}$$

By taking $\Sigma_l(z, t) = \frac{g_l(z, t)}{f(z, t)}$, $l = 1, 2$ and inserting it into Eq. (1.1), one obtains bilinear form. According to above process, the below Theorem will be considered.

Theorem 2.3 *By the below issues, one gets*

$$\Sigma_l(z, t) = \frac{g_l(z, t)}{f(z, t)}, \quad l = 1, 2, \tag{2.14}$$

where $g_l, l = 1, 2$ are the complex functions and f is a real function. Plugging the above solution (2.14) into Eq. (1.1), we arrive at the bilinear equations as below

$$\left(iD_z + \Lambda D_z^2 + \frac{1}{2} D_t^2 \right) (g_l, f) = 0,$$

$$\left(\Lambda D_z^2 + \frac{1}{2} D_t^2 \right) (f, f) = \delta \sum_{l=1}^2 g_l g_l^*, \tag{2.15}$$

where $*$ shows the complex conjugate and D denotes the Hirota’s bilinear operator which manages with respect to the functions of z and t . The bilinear definitions for operator are

$$\begin{aligned}
 D_z(g_l f) &= \frac{\partial g_l}{\partial z} f - g_l \frac{\partial f}{\partial z}, \\
 D_z^2(g_l f) &= \frac{\partial^2 g_l}{\partial z^2} f - 2 \frac{\partial g_l}{\partial z} \frac{\partial f}{\partial z} + g_l \frac{\partial^2 f}{\partial z^2}, \\
 D_t^2(g_l f) &= \frac{\partial^2 g_l}{\partial t^2} f - 2 \frac{\partial g_l}{\partial t} \frac{\partial f}{\partial t} + g_l \frac{\partial^2 f}{\partial t^2}, \\
 D_z^2(f f) &= 2f \frac{\partial^2 f}{\partial z^2} - 2\left(\frac{\partial f}{\partial z}\right)^2, \\
 D_t^2(f f) &= 2f \frac{\partial^2 f}{\partial t^2} - 2\left(\frac{\partial f}{\partial t}\right)^2.
 \end{aligned}
 \tag{2.16}$$

3 Solitary wave solutions

In this section according to the rational transformation (2.14) the following cases will be analyzed as:

3.1 Nonparaxial soliton solutions

By supposing the below function

$$\begin{aligned}
 f(z, t) &= h_1 \sin(b_1 \zeta_1) \exp(b_2 \zeta_2), \quad g_l(z, t) = m_l \exp(ic_l \zeta_{l+2}), \quad l = 1, 2, \\
 \zeta_l &= \lambda_l z + \mu_l(t) + \xi_l, \quad l = 1, 2, 3, 4.
 \end{aligned}
 \tag{3.1}$$

Afterwards, inserting $\Sigma_l = g_l(z, t)/f(z, t)$, $l = l, 2$ Eq. (2.15) and using relations (2.16) and taking the coefficients of the nonlinear expressions to zero, yield a system of algebraic equations including below:

$$\begin{aligned}
 &4 i \Lambda b_1 c_1 \lambda_1 \lambda_3 - 4 \Lambda b_1 b_2 \lambda_1 \lambda_2 \\
 &\quad + 2 i b_1 c_1 \mu_1 \mu_3 - 2 b_1 \mu_1 b_2 \mu_2 + 2 i b_1 \lambda_1 = 0, \\
 &4 i \Lambda b_2 c_1 \lambda_2 \lambda_3 + 2 \Lambda b_1^2 \lambda_1^2 - 2 \Lambda b_2^2 \lambda_2^2 \\
 &\quad + 2 \Lambda c_1^2 \lambda_3^2 + 2 i b_2 c_1 \mu_2 \mu_3 + b_1^2 \mu_1^2 - b_2^2 \mu_2^2 \\
 &\quad + c_1^2 \mu_3^2 + 2 i b_2 \lambda_2 + 2 c_1 \lambda_3 = 0, \\
 &4 i \Lambda n_1 b_1 c_2 \lambda_1 \lambda_4 - 4 \Lambda b_1 b_2 \lambda_1 \lambda_2 n_1 \\
 &\quad + 2 i n_1 b_1 c_2 \mu_1 \mu_4 - 2 b_1 \mu_1 b_2 \mu_2 n_1 + 2 i b_1 \lambda_1 n_1 = 0, \\
 &4 i \Lambda b_2 c_2 \lambda_2 \lambda_4 + 2 \Lambda b_1^2 \lambda_1^2 - 2 \Lambda b_2^2 \lambda_2^2 \\
 &\quad + 2 \Lambda c_2^2 \lambda_4^2 + 2 i b_2 c_2 \mu_2 \mu_4 + b_1^2 \mu_1^2 - b_2^2 \mu_2^2 + c_2^2 \mu_4^2 + 2 i b_2 \lambda_2 + 2 c_2 \lambda_4 = 0, \\
 &4 i \Lambda b_2 c_2 \lambda_2 \lambda_4 n_2 + 2 \Lambda b_1^2 \lambda_1^2 n_2 \\
 &\quad - 2 \Lambda b_2^2 \lambda_2^2 n_2 + 2 \Lambda c_2^2 \lambda_4^2 n_2 + 2 i b_2 c_2 \mu_2 \mu_4 n_2 \\
 &\quad + b_1^2 \mu_1^2 n_2 - b_2^2 \mu_2^2 n_2 + c_2^2 \mu_4^2 n_2 + \\
 &2 i b_2 \lambda_2 n_2 + 2 c_2 \lambda_4 n_2 + 4 i \Lambda n_1 b_1 c_2 \lambda_1 \lambda_4 - 4 \Lambda b_1 b_2 \lambda_1 \lambda_2 n_1 + 2 i n_1 b_1 c_2 \mu_1 \mu_4 \\
 &\quad - 2 b_1 \mu_1 b_2 \mu_2 n_1 + 2 i b_1 \lambda_1 n_1 = 0.
 \end{aligned}$$

By solving the above equations get the following results:

3.1.1 Set I solutions

$$\begin{aligned}
 b_1 &= \frac{\sqrt{2(2(i\Lambda\lambda_4c_2 - \Lambda b_2\lambda_2 + i)\lambda_1^2 + (ic_2\lambda_4 - b_2\lambda_2)\mu_1^2)\Lambda(ic_2\lambda_4 - b_2\lambda_2) + 2i(ic_2\lambda_4 - b_2\lambda_2)\mu_1^2 - \lambda_1^2}}{\mu_1\sqrt{2\Lambda\lambda_1^2 + \mu_1^2}}, \\
 \lambda_3 &= \frac{i(i\Lambda\lambda_4c_2 - 2\Lambda b_2\lambda_2 + i)}{\Lambda c_1}, \quad \mu_3 = \frac{-i(2i\Lambda\lambda_1\lambda_4c_2 - 2\Lambda b_2\lambda_1\lambda_2 + b_2\mu_1\mu_2 + i\lambda_1)}{\mu_1 c_1}, \\
 \mu_4 &= \frac{i(2i\Lambda\lambda_1\lambda_4c_2 - 2\Lambda b_2\lambda_1\lambda_2 - b_2\mu_1\mu_2 + i\lambda_1)}{\mu_1 c_2}.
 \end{aligned}
 \tag{3.2}$$

Then, the solution is

$$\begin{aligned}
 \Sigma_l(z, t) &= \frac{m_l \exp(ic_l \zeta_{l+2})}{h_l \sin(b_l \zeta_1) \exp(b_2 \zeta_2)}, \quad l = 1, 2, \\
 \zeta_k &= \lambda_k z + \mu_k(t) + \xi_k, \quad k = 1, 2, 3, 4.
 \end{aligned}
 \tag{3.3}$$

Further, the following analysis can be extended to explore multiple soliton dynamics on arbitrary backgrounds in a straightforward manner. Figure 1 depicts the impact of treatment of singular soliton solution where graphs of $\Sigma_l, l = 1, 2$ are given with the following chosen values

$$\begin{aligned}
 \Lambda &= 0.1e - 2, \delta = 1, \lambda_1 = 1, \lambda_2 = 1, \\
 \lambda_4 &= 1, c_1 = 1, c_2 = 2, b_1 = 1, b_2 = 2.5, h_1 = 1, \\
 \mu_1 &= 1, m_1 = 2, \mu_2 = 2, \mu_4 = 3, \xi_1 = 1, \xi_2 = 1, \xi_3 = 2.5,
 \end{aligned}
 \tag{3.4}$$

$$\Sigma_1 = 2 \frac{e^{-0.0050000000000000t + 1.0040000000it + 2.5000000000z - 1002.0iz - 2.5000000000 + 2.5000000000i}}{\sin((1.021552097 - 2.457045519i)(t + z + 1))}, \tag{3.5}$$

$$\begin{aligned}
 \Lambda &= 0.1e - 2, \delta = 1, \lambda_1 = 1, \lambda_2 = 1, \\
 \lambda_4 &= 1, c_1 = 1, c_2 = 2, b_1 = 1, b_2 = 2.5, h_1 = 1, \\
 \mu_1 &= 1, m_2 = 2, \mu_2 = 2, \mu_4 = 3, \xi_1 = 1, \xi_2 = 1, \xi_4 = 2.5,
 \end{aligned}
 \tag{3.6}$$

$$\Sigma_2 = 2 \frac{e^{0.0050t - 1.004it + 2iz - 2.5 + 5.0i - 2.5z}}{\sin((1.021552097 - 2.457045519i)(t + z + 1))}, \tag{3.7}$$

in Eq. (3.3). We investigate the dynamics of general nonparaxial solitons received from the Hirota bilinear technique, which is presented in Fig. 1. From the figure, it is apparent that the solitons exhibit a stable propagation in both components of CNLH system as shown in Figs. 1.

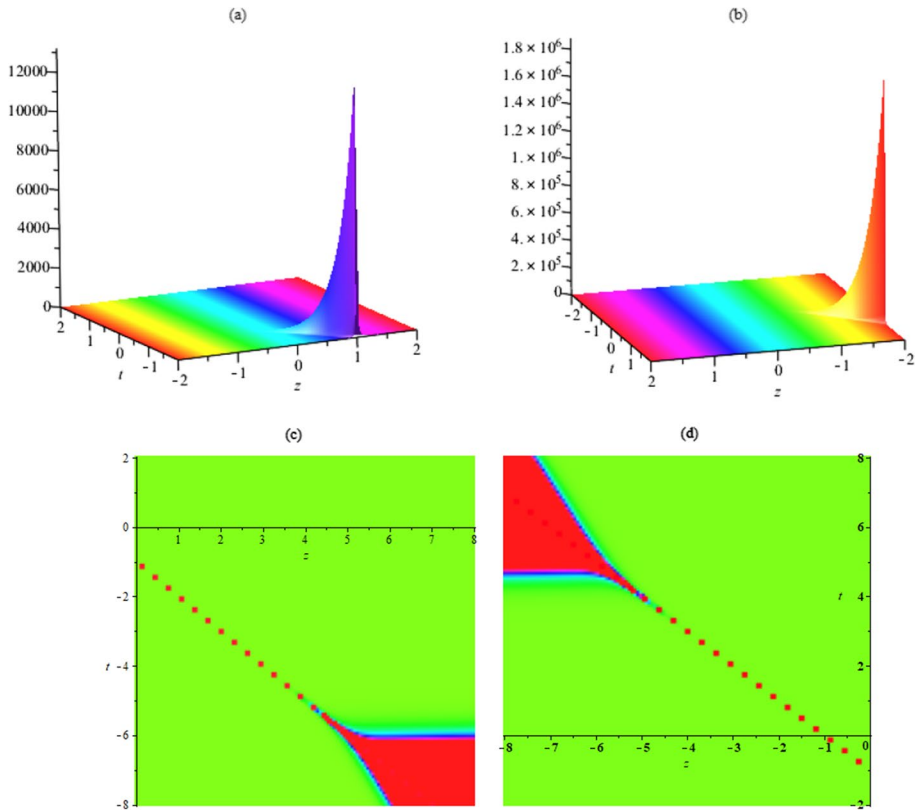


Fig. 1 Plot of soliton solution (3.3) ($|\Sigma_l|^2$) such as left graphs $|\Sigma_1|^2$ and right graphs $|\Sigma_2|^2$

3.1.2 Set II solutions

$$\begin{aligned}
 b_1 &= \frac{\sqrt{2(2i\Lambda\lambda_1^2\lambda_4c_2 - 2\Lambda b_2\lambda_1^2\lambda_2 + ic_2\lambda_4\mu_1^2 - b_2\lambda_2\mu_1^2 + 2i\lambda_1^2)\Lambda(ic_2\lambda_4 - b_2\lambda_2) - 2ib_2\lambda_2\mu_1^2 - 2c_2\lambda_4\mu_1^2 - \lambda_1^2}}{\sqrt{2\Lambda\lambda_1^2 + \mu_1^2\mu_1}}, \\
 \lambda_3 &= \frac{c_2\lambda_4}{c_1}, \quad \mu_3 = \frac{i(2i\Lambda\lambda_1\lambda_4c_2 - 2\Lambda b_2\lambda_1\lambda_2 - b_2\mu_1\mu_2 + i\lambda_1)}{\mu_1c_1}, \quad \mu_4 = \frac{i(2i\Lambda\lambda_1\lambda_4c_2 - 2\Lambda b_2\lambda_1\lambda_2 - b_2\mu_1\mu_2 + i\lambda_1)}{\mu_1c_2}.
 \end{aligned}
 \tag{3.8}$$

Then, the solution is

$$\begin{aligned}
 \Sigma_l(z, t) &= \frac{m_l \exp(ic_l \zeta_{l+2})}{h_1 \sin(b_1 \zeta_1) \exp(b_2 \zeta_2)}, \quad l = 1, 2, \\
 \zeta_k &= \lambda_k z + \mu_k(t) + \xi_k, \quad k = 1, 2, 3, 4.
 \end{aligned}
 \tag{3.9}$$

Figure 2 depicts the impact of treatment of singular soliton solution where graphs of $\Sigma_l, l = 1, 2$ are given with the following parameters

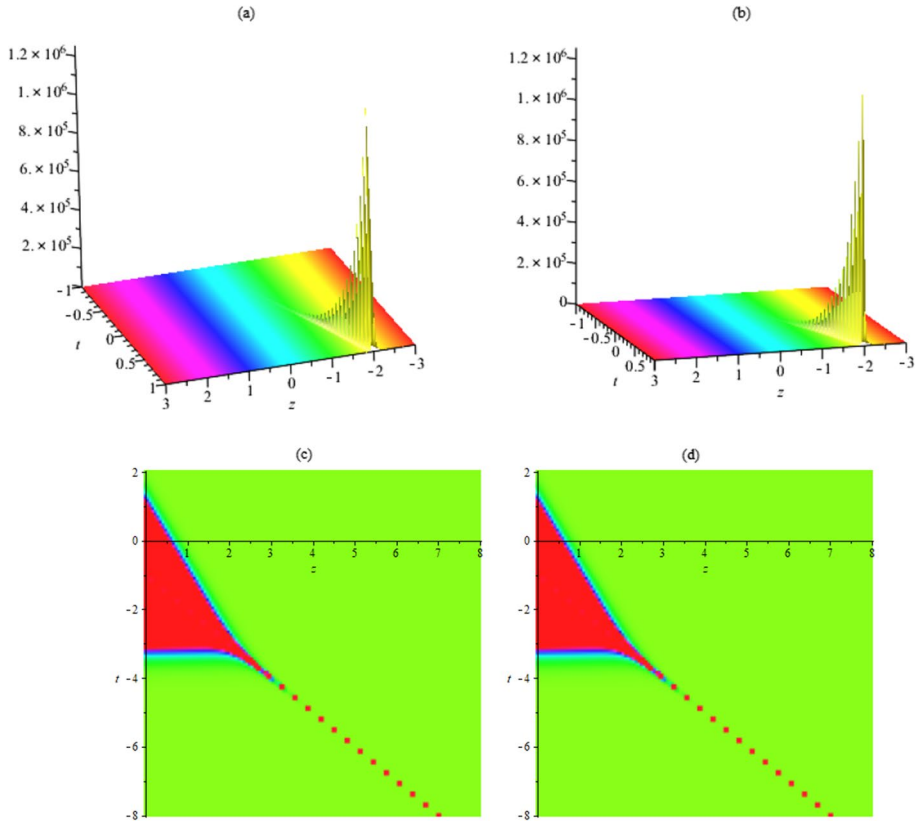


Fig. 2 Plot of soliton solution (3.8) ($|\Sigma_1|^2$) such as left graphs $|\Sigma_1|^2$ and right graphs $|\Sigma_2|^2$

$$\Lambda = 0.1e - 2, \delta = 1, \lambda_1 = 1, \lambda_2 = 1, \lambda_4 = 1, c_1 = 1, c_2 = 2, b_1 = 1, b_2 = 2.5, h_1 = 1, \mu_1 = 1, m_1 = 2, \mu_2 = 2, \mu_4 = 3, \xi_1 = 1, \xi_2 = 1, \xi_3 = 2.5, \tag{3.10}$$

$$\Sigma_1 = 2 \frac{e^{0.0050t - 1.004it + 2iz - 2.5 + 2.5i - 2.5z}}{\sin((1.021552097 - 2.457045519i)(t + z + 1))}, \tag{3.11}$$

$$\Lambda = 0.1e - 2, \delta = 1, \lambda_1 = 1, \lambda_2 = 1, \lambda_4 = 1, c_1 = 1, c_2 = 2, b_1 = 1, b_2 = 2.5, h_1 = 1, \mu_1 = 1, m_2 = 2, \mu_2 = 2, \mu_4 = 3, \xi_1 = 1, \xi_2 = 1, \xi_4 = 2.5, \tag{3.12}$$

$$\Sigma_2 = 2 \frac{e^{0.0050t - 1.004it + 2iz - 2.5 + 5.0i - 2.5z}}{\sin((1.021552097 - 2.457045519i)(t + z + 1))}, \tag{3.13}$$

in Eq. (3.8). We investigate the dynamics of general nonparaxial solitons received from the Hirota bilinear technique, which is presented in Fig. 2. From the figure, it is apparent that the solitons exhibit a stable propagation in both components of CNLH system as shown in Figs. 2.

3.1.3 Set III solutions

$$\Sigma_1 = \frac{m_1 e^{-1/2 \frac{-2\Lambda ib_2 \mu_2 + 2i\Lambda ic_2 \mu_4 - 2i\Lambda c_1 \xi_3 + 2b_2 \xi_2 \Lambda + iz}{\Lambda}}}{h_1 \sin \left(1/2 \frac{\sqrt{1 - 4ib_2 c_2 \mu_2 \mu_4 \Lambda + 2b_2^2 \mu_2^2 \Lambda - 2c_2^2 \mu_4^2 \Lambda} (z\lambda_1 + \xi_1)}{\lambda_1 \Lambda} \right)}, \tag{3.14}$$

$$\Sigma_2 = \frac{m_2 e^{1/2 \frac{2i\Lambda ic_2 \mu_4 + 2i\Lambda c_2 \xi_4 - 2\Lambda ib_2 \mu_2 - 2b_2 \xi_2 \Lambda - iz}{\Lambda}}}{h_1 \sin \left(1/2 \frac{\sqrt{1 - 4ib_2 c_2 \mu_2 \mu_4 \Lambda + 2b_2^2 \mu_2^2 \Lambda - 2c_2^2 \mu_4^2 \Lambda} (z\lambda_1 + \xi_1)}{\lambda_1 \Lambda} \right)}. \tag{3.15}$$

3.2 Singular soliton solutions

Supposing the below function

$$\begin{aligned} f(z, t) &= h_1 \sinh(b_1 \zeta_1), \quad g_l(z, t) = m_l \exp(ic_l \zeta_{l+1}), \quad l = 1, 2, \\ \zeta_l &= \lambda_l z + \mu_l(t) + \xi_l, \quad l = 1, 2, 3. \end{aligned} \tag{3.16}$$

Afterwards, inserting $\Sigma_l = g_l(z, t)/f(z, t)$, $l = 1, 2$ Eq. (2.15) and using relations (2.16) and taking the coefficients of the nonlinear expressions to zero, yield a system of algebraic equations including below:

$$\begin{aligned} -4i\Lambda c_1 \lambda_2 b_1 \lambda_1 - 2ic_1 \mu_2 b_1 \mu_1 - 2ib_1 \lambda_1 &= 0, \\ 2\Lambda b_1^2 \lambda_1^2 - 2\Lambda c_1^2 \lambda_2^2 + b_1^2 \mu_1^2 - c_1^2 \mu_2^2 - 2c_1 \lambda_2 &= 0, \\ -4i\Lambda c_2 \lambda_3 b_1 \lambda_1 - 2ic_2 \mu_3 b_1 \mu_1 - 2ib_1 \lambda_1 &= 0, \\ 2\Lambda b_1^2 \lambda_1^2 - 2\Lambda c_2^2 \lambda_3^2 + b_1^2 \mu_1^2 - c_2^2 \mu_3^2 - 2c_2 \lambda_3 &= 0. \end{aligned}$$

Also, by solving $-2\Lambda b_1^2 h_1^2 \lambda_1^2 - h_1^2 b_1^2 \mu_1^2 - (|m_1|)^2 \delta - (|m_2|)^2 \delta = 0$ we can get to the amplitude of solitary wave as below

$$h_1 = \pm \frac{\sqrt{-(2\Lambda \lambda_1^2 + \mu_1^2) \delta \left((|m_1|)^2 + (|m_2|)^2 \right)}}{(2\Lambda \lambda_1^2 + \mu_1^2) b_1}. \tag{3.17}$$

By solving the above equations get the following results:

3.2.1 Set I solutions

$$\begin{aligned}
 \lambda_1 &= \frac{\sqrt{-(4\Lambda^2 c_2^2 \lambda_3^2 - 2\Lambda b_1^2 \mu_1^2 + 4\Lambda c_2 \lambda_3 + 1)(2\Lambda c_2^2 \lambda_3^2 - b_1^2 \mu_1^2 + 2c_2 \lambda_3) \mu_1}}{4\Lambda^2 c_2^2 \lambda_3^2 - 2\Lambda b_1^2 \mu_1^2 + 4\Lambda c_2 \lambda_3 + 1}, \\
 \lambda_2 &= \frac{c_2 \lambda_3}{c_1}, \\
 \mu_2 &= -\frac{\sqrt{-(4\Lambda^2 c_2^2 \lambda_3^2 - 2\Lambda b_1^2 \mu_1^2 + 4\Lambda c_2 \lambda_3 + 1)(2\Lambda c_2^2 \lambda_3^2 - b_1^2 \mu_1^2 + 2c_2 \lambda_3)(2\Lambda c_2 \lambda_3 + 1)}}{(4\Lambda^2 c_2^2 \lambda_3^2 - 2\Lambda b_1^2 \mu_1^2 + 4\Lambda c_2 \lambda_3 + 1)c_1}, \\
 \mu_3 &= -\frac{\sqrt{-(4\Lambda^2 c_2^2 \lambda_3^2 - 2\Lambda b_1^2 \mu_1^2 + 4\Lambda c_2 \lambda_3 + 1)(2\Lambda c_2^2 \lambda_3^2 - b_1^2 \mu_1^2 + 2c_2 \lambda_3)(2\Lambda c_2 \lambda_3 + 1)}}{(4\Lambda^2 c_2^2 \lambda_3^2 - 2\Lambda b_1^2 \mu_1^2 + 4\Lambda c_2 \lambda_3 + 1)c_2}.
 \end{aligned}
 \tag{3.18}$$

Then, the solution is

$$\begin{aligned}
 \Sigma_l(z, t) &= \frac{m_l}{h_1} \exp(ic_l \zeta_{l+1}) \operatorname{csch}(b_1 \zeta_1), \\
 l &= 1, 2, \quad \zeta_k = \lambda_k z + \mu_k(t) + \xi_k, \quad k = 1, 2, 3.
 \end{aligned}
 \tag{3.19}$$

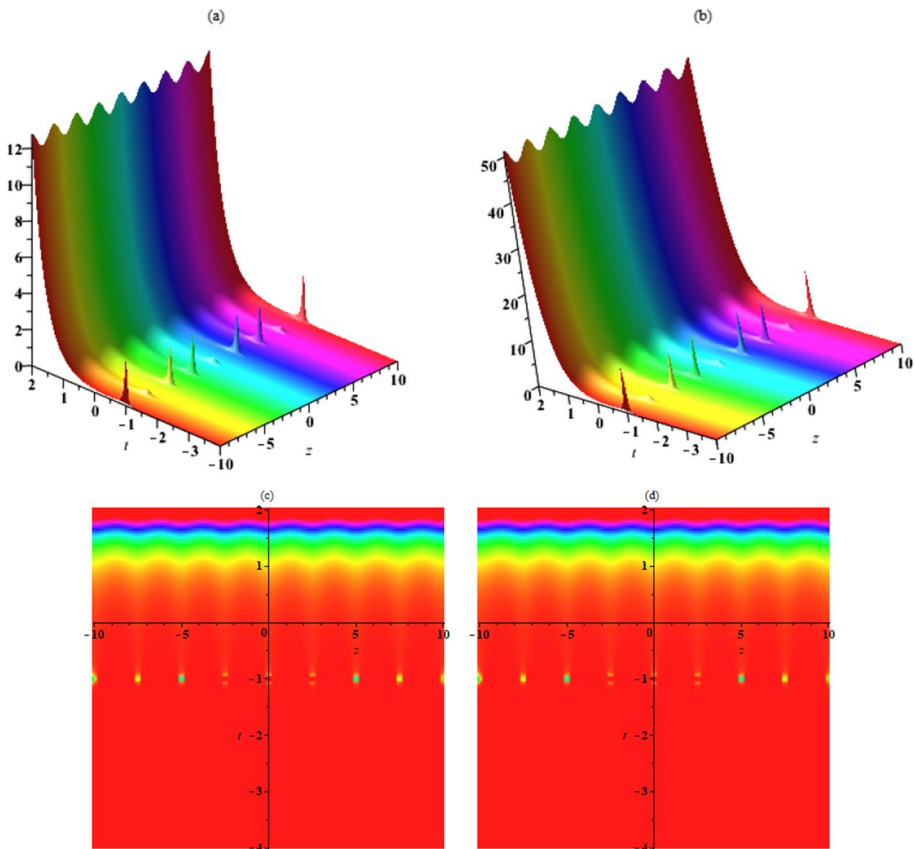


Fig. 3 Plot of soliton solution (3.19) ($|\Sigma_l|^2$) such as left graphs $|\Sigma_1|^2$ and right graphs $|\Sigma_2|^2$

Figure 3 depicts the impact of analysis of singular soliton solution where graphs of $\Sigma_l, l = 1, 2$ are given with the following parameters

$$\begin{aligned} \Lambda &= 0.1e - 2, \delta = -1, \lambda_3 = 1, c_1 = 1, c_2 = 2, b_1 \\ &= \frac{2}{3}, m_1 = 2, \mu_2 = 2, \mu_1 = 1, \xi_1 = 1, \xi_2 = 1, \xi_3 = 2.5, \end{aligned} \tag{3.20}$$

$$\Sigma_1 = 0.6643035869 \frac{e^{i(-1.888571085 it+2z+1)}}{\sqrt{(|1|)^2 + (|2|)^2 \sinh(2/3 t + 1.254031265 iz + 2/3)}}, \tag{3.21}$$

$$\begin{aligned} \Lambda &= 0.1e - 2, \delta = -1, \lambda_3 = 1, c_1 = 1, c_2 = 2, \\ b_1 &= \frac{2}{3}, m_1 = 2, \mu_2 = 2, \mu_1 = 1, \xi_1 = 1, \xi_2 = 1, \xi_3 = 2.5, \end{aligned} \tag{3.22}$$

$$\Sigma_2 = 1.328607174 \frac{e^{2i(-0.9442855426 it+z+2.5)}}{\sqrt{(|1|)^2 + (|2|)^2 \sinh(2/3 t + 1.254031265 iz + 2/3)}}, \tag{3.23}$$

in Eq. (3.19). We investigate the dynamics of general nonparaxial solitons received from the Hirota bilinear technique, which is presented in Fig. 3. From the figure, it is apparent that the solitons exhibit a stable propagation in both components of CNLH system as shown in Figs. 3.

3.2.2 Set II solutions

$$\begin{aligned} \lambda_1 &= \frac{\sqrt{-(4\Lambda^2 c_2^2 \lambda_3^2 - 2\Lambda b_1^2 \mu_1^2 + 4\Lambda c_2 \lambda_3 + 1)(2\Lambda c_2^2 \lambda_3^2 - b_1^2 \mu_1^2 + 2c_2 \lambda_3) \mu_1}}{4\Lambda^2 c_2^2 \lambda_3^2 - 2\Lambda b_1^2 \mu_1^2 + 4\Lambda c_2 \lambda_3 + 1}, \\ \lambda_2 &= -\frac{\Lambda c_2 \lambda_3 + 1}{\Lambda c_1}, \\ \mu_2 &= \frac{\sqrt{-(4\Lambda^2 c_2^2 \lambda_3^2 - 2\Lambda b_1^2 \mu_1^2 + 4\Lambda c_2 \lambda_3 + 1)(2\Lambda c_2^2 \lambda_3^2 - b_1^2 \mu_1^2 + 2c_2 \lambda_3)(2\Lambda c_2 \lambda_3 + 1)}}{(4\Lambda^2 c_2^2 \lambda_3^2 - 2\Lambda b_1^2 \mu_1^2 + 4\Lambda c_2 \lambda_3 + 1)c_1}, \\ \mu_3 &= -\frac{\sqrt{-(4\Lambda^2 c_2^2 \lambda_3^2 - 2\Lambda b_1^2 \mu_1^2 + 4\Lambda c_2 \lambda_3 + 1)(2\Lambda c_2^2 \lambda_3^2 - b_1^2 \mu_1^2 + 2c_2 \lambda_3)(2\Lambda c_2 \lambda_3 + 1)}}{(4\Lambda^2 c_2^2 \lambda_3^2 - 2\Lambda b_1^2 \mu_1^2 + 4\Lambda c_2 \lambda_3 + 1)c_2}. \end{aligned} \tag{3.24}$$

Then, the solution is

$$\begin{aligned} \Sigma_l(z, t) &= \frac{m_l}{h_l} \exp(ic_l \zeta_{l+1}) \operatorname{csch}(b_l \zeta_l), \\ l &= 1, 2, \quad \zeta_k = \lambda_k z + \mu_k(t) + \xi_k, \quad k = 1, 2, 3. \end{aligned} \tag{3.25}$$

Figure 4 depicts the impact of analysis of singular soliton solution where graphs of $\Sigma_l, l = 1, 2$ are given with the following chosen parameters

$$\begin{aligned} \Lambda &= 0.1e - 2, \delta = -1, \lambda_3 = 1, c_1 = 1, c_2 = 2, b_1 \\ &= \frac{4}{3}, m_1 = 2, \mu_2 = 2, \mu_1 = 1, \xi_1 = 1, \xi_2 = 1, \xi_3 = 2.5, \end{aligned} \tag{3.26}$$

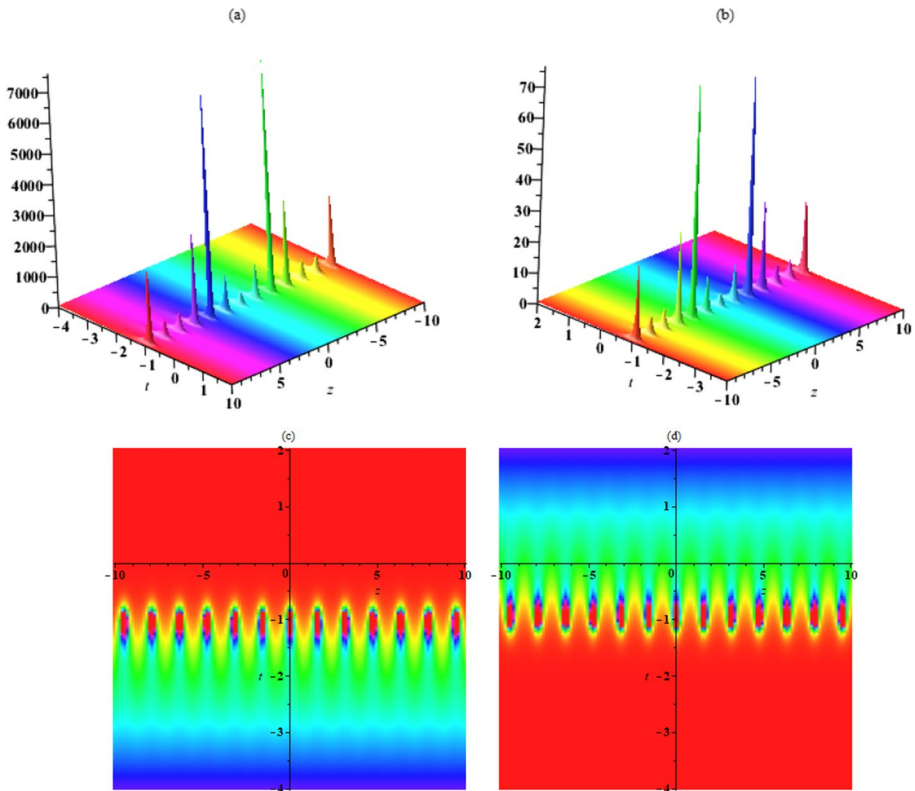


Fig. 4 Plot of soliton solution (3.24) ($|\Sigma_1|^2$) such as left graphs $|\Sigma_1|^2$ and right graphs $|\Sigma_2|^2$

$$\Sigma_1 = 1.330369615 \frac{e^{i(1.496033653 it - 1002.0 z + 1)}}{\sqrt{(|1|^2 + |2|^2) \sinh(4/3 t + 1.986764478 iz + 4/3)}}, \tag{3.27}$$

$$\Lambda = 0.1e - 2, \delta = -1, \lambda_3 = 1, c_1 = 1, c_2 = 2, b_1 = \frac{4}{3}, \tag{3.28}$$

$$m_1 = 2, \mu_2 = 2, \mu_1 = 1, \xi_1 = 1, \xi_2 = 1, \xi_3 = 2.5,$$

$$\Sigma_2 = 2.660739229 \frac{e^{2i(-0.7480168264 it + z + 2.5)}}{\sqrt{(|1|^2 + |2|^2) \sinh(4/3 t + 1.986764478 iz + 4/3)}}, \tag{3.29}$$

in Eq. (3.24). We investigate the dynamics of general nonparaxial solitons received from the Hirota bilinear technique, which is presented in Fig. 4. From the figure, it is apparent that the solitons exhibit a stable propagation in both components of CNLH system as shown in Figs. 4.

3.2.3 Set III solutions

$$\Sigma_1 = \frac{m_1 e^{ic_1 \left(\frac{\mu_3 c_2}{c_1} - 1/2 \frac{z}{c_1 \Lambda} + \xi_2 \right)} \sqrt{2} \sqrt{\Lambda \lambda_1^2} b_1}{\sqrt{-\delta \left((|m_1|)^2 + (|m_2|)^2 \right)} \sinh \left(b_1 \left(1/2 \frac{z \sqrt{2 \Lambda c_2^2 \mu_3^2 - 1}}{b_1 \Lambda} + \xi_1 \right) \right)}, \tag{3.30}$$

$$\Sigma_2 = \frac{m_2 e^{ic_2 \left(\mu_3 - 1/2 \frac{z}{c_2 \Lambda} + \xi_3 \right)} \sqrt{2} \sqrt{\Lambda \lambda_1^2} b_1}{\sqrt{-\delta \left((|m_1|)^2 + (|m_2|)^2 \right)} \sinh \left(b_1 \left(1/2 \frac{z \sqrt{2 \Lambda c_2^2 \mu_3^2 - 1}}{b_1 \Lambda} + \xi_1 \right) \right)}. \tag{3.31}$$

3.3 Bright soliton solutions

Supposing bright soliton solutions as the below function

$$\begin{aligned} f(z, t) &= h_1 \cosh(b_1 \zeta_l), \quad g_l(z, t) = m_l \exp(ic_l \zeta_{l+1}), \\ l &= 1, 2, \quad \zeta_l = \lambda_l z + \mu_l(t) + \xi_l, \quad l = 1, 2, 3. \end{aligned} \tag{3.32}$$

By putting $\Sigma_l = g_l(z, t)/f(z, t)$, $l = 1, 2$ Eq. (2.15) and using relations (2.16) and taking the coefficients of the nonlinear expressions to zero, yield a system of algebraic equations including below:

$$\begin{aligned} 2 \Lambda b_1^2 \lambda_1^2 - 2 \Lambda c_1^2 \lambda_2^2 + b_1^2 \mu_1^2 - c_1^2 \mu_2^2 - 2 c_1 \lambda_2 &= 0, \\ -4 i \Lambda c_1 \lambda_2 b_1 \lambda_1 - 2 ic_1 \mu_2 b_1 \mu_1 - 2 ib_1 \lambda_1 &= 0, \\ 2 \Lambda b_1^2 \lambda_1^2 - 2 \Lambda c_2^2 \lambda_3^2 + b_1^2 \mu_1^2 - c_2^2 \mu_3^2 - 2 c_2 \lambda_3 &= 0, \\ -4 i \Lambda c_2 \lambda_3 b_1 \lambda_1 - 2 ic_2 \mu_3 b_1 \mu_1 - 2 ib_1 \lambda_1 &= 0. \end{aligned}$$

Also, by solving $2 \Lambda b_1^2 h_1^2 \lambda_1^2 + h_1^2 b_1^2 \mu_1^2 - (|m_1|)^2 \delta - (|m_2|)^2 \delta = 0$ we can get to the amplitude of solitary wave as below

$$h_1 = \pm \frac{\sqrt{(2 \Lambda \lambda_1^2 + \mu_1^2) \delta \left((|m_1|)^2 + (|m_2|)^2 \right)}}{(2 \Lambda \lambda_1^2 + \mu_1^2) b_1}. \tag{3.33}$$

Therefore, the form of solutions is as below

$$\Sigma_l = \pm \frac{m_l (2 \Lambda \lambda_1^2 + \mu_1^2) b_1}{\sqrt{(2 \Lambda \lambda_1^2 + \mu_1^2) \delta \left((|m_1|)^2 + (|m_2|)^2 \right)}} \exp(ic_l \zeta_{l+1}) \operatorname{sech}(b_1 \zeta_l), \quad l = 1, 2. \tag{3.34}$$

By solving the above equations get the following results:

3.3.1 Set I solutions

$$\begin{aligned} \lambda_1 &= \frac{\sqrt{-(4\Lambda^2 c_2^2 \lambda_3^2 - 2\Lambda b_1^2 \mu_1^2 + 4\Lambda c_2 \lambda_3 + 1)(2\Lambda c_2^2 \lambda_3^2 - b_1^2 \mu_1^2 + 2c_2 \lambda_3) \mu_1}}{4\Lambda^2 c_2^2 \lambda_3^2 - 2\Lambda b_1^2 \mu_1^2 + 4\Lambda c_2 \lambda_3 + 1}, \\ \lambda_2 &= \frac{c_2 \lambda_3}{c_1}, \\ \mu_2 &= -\frac{\sqrt{-(4\Lambda^2 c_2^2 \lambda_3^2 - 2\Lambda b_1^2 \mu_1^2 + 4\Lambda c_2 \lambda_3 + 1)(2\Lambda c_2^2 \lambda_3^2 - b_1^2 \mu_1^2 + 2c_2 \lambda_3)(2\Lambda c_2 \lambda_3 + 1)}}{(4\Lambda^2 c_2^2 \lambda_3^2 - 2\Lambda b_1^2 \mu_1^2 + 4\Lambda c_2 \lambda_3 + 1)c_1}, \\ \mu_3 &= -\frac{\sqrt{-(4\Lambda^2 c_2^2 \lambda_3^2 - 2\Lambda b_1^2 \mu_1^2 + 4\Lambda c_2 \lambda_3 + 1)(2\Lambda c_2^2 \lambda_3^2 - b_1^2 \mu_1^2 + 2c_2 \lambda_3)(2\Lambda c_2 \lambda_3 + 1)}}{(4\Lambda^2 c_2^2 \lambda_3^2 - 2\Lambda b_1^2 \mu_1^2 + 4\Lambda c_2 \lambda_3 + 1)c_2}. \end{aligned} \tag{3.35}$$

Then, the solution is

$$\begin{aligned} \Sigma_l(z, t) &= \frac{m_l}{h_1} \exp(ic_l \zeta_{l+1}) \operatorname{sech}(b_l \zeta_l), \quad l = 1, 2, \\ \zeta_k &= \lambda_k z + \mu_k(t) + \xi_k, \quad k = 1, 2, 3. \end{aligned} \tag{3.36}$$

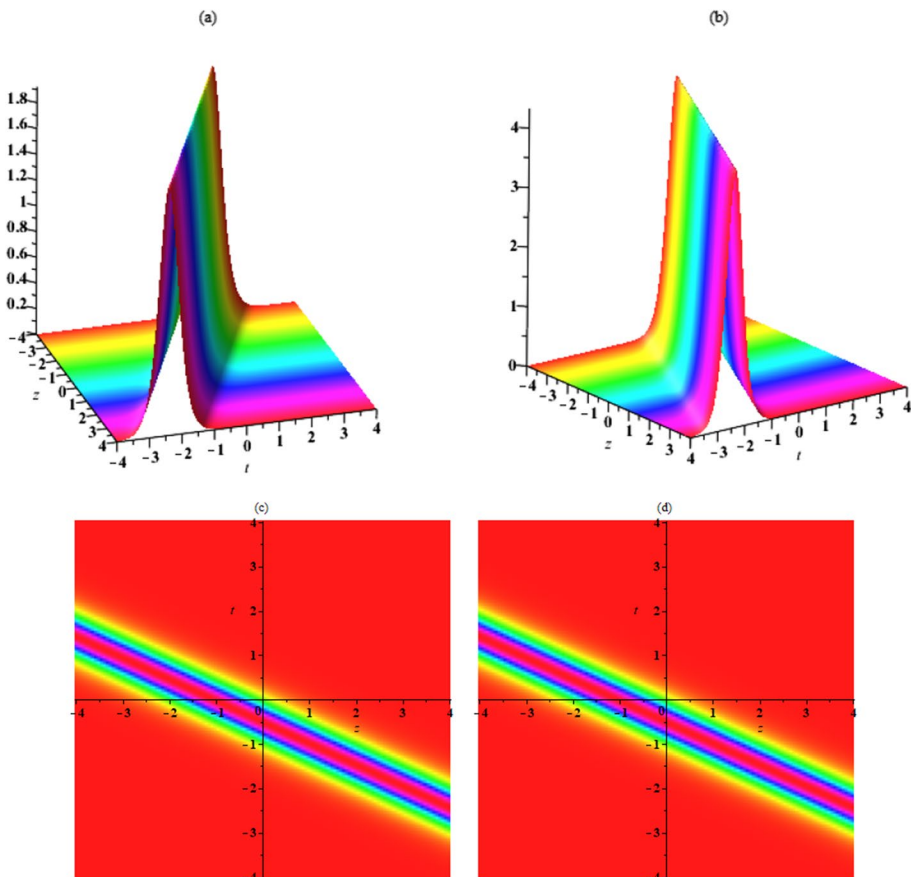


Fig. 5 Plot of bright soliton solution (3.36) ($|\Sigma_l|^2$) such as left graphs $|\Sigma_1|^2$ and right graphs $|\Sigma_2|^2$

Figure 5 depicts the impact of analysis bright soliton solution where graphs of $\Sigma_l, l = 1, 2$ are given with the following values

$$\begin{aligned} \Lambda &= 0.1e - 2, \delta = 1, \lambda_3 = 1, c_1 = 2, c_2 = 3, b_1 = \frac{5}{4}, \\ m_1 &= 2, m_2 = 3, \mu_1 = 2, \xi_1 = 1, \xi_2 = 1, \xi_3 = 2.5, \end{aligned} \tag{3.37}$$

$$\Sigma_1 = 5.001160405 \frac{e^{2i(-0.2423331108t+3/2z+1)}}{\sqrt{(|2|)^2 + (|3|)^2 \cosh(5/2t + 1.204438920z + 5/4)}}, \tag{3.38}$$

$$\begin{aligned} \Lambda &= 0.1e - 2, \delta = 1, \lambda_3 = 1, c_1 = 2, c_2 = 3, b_1 \\ &= \frac{5}{4}, m_1 = 2, m_2 = 3, \mu_1 = 2, \xi_1 = 1, \xi_2 = 1, \xi_3 = 2.5, \end{aligned} \tag{3.39}$$

$$\Sigma_2 = 7.501740608 \frac{e^{3i(-0.1615554072t+z+2.5)}}{\sqrt{(|2|)^2 + (|3|)^2 \cosh(5/2t + 1.204438920z + 5/4)}}, \tag{3.40}$$

in Eq. (3.36). We investigate the dynamics of general bright solitons received from the Hirota bilinear technique, which is presented in Fig. 5. From the figure, it is apparent that the solitons exhibit a stable propagation in both components of CNLH system as shown in Figs. 5.

3.3.2 Set II solutions

$$\begin{aligned} \lambda_1 &= \frac{\sqrt{-(4\Lambda^2c_2^2\lambda_3^2 - 2\Lambda b_1^2\mu_1^2 + 4\Lambda c_2\lambda_3 + 1)(2\Lambda c_2^2\lambda_3^2 - b_1^2\mu_1^2 + 2c_2\lambda_3)\mu_1}}{4\Lambda^2c_2^2\lambda_3^2 - 2\Lambda b_1^2\mu_1^2 + 4\Lambda c_2\lambda_3 + 1}, \\ \lambda_2 &= -\frac{\Lambda c_2\lambda_3 + 1}{\Lambda c_1}, \\ \mu_2 &= -\frac{\sqrt{-(4\Lambda^2c_2^2\lambda_3^2 - 2\Lambda b_1^2\mu_1^2 + 4\Lambda c_2\lambda_3 + 1)(2\Lambda c_2^2\lambda_3^2 - b_1^2\mu_1^2 + 2c_2\lambda_3)(2\Lambda c_2\lambda_3 + 1)}}{(4\Lambda^2c_2^2\lambda_3^2 - 2\Lambda b_1^2\mu_1^2 + 4\Lambda c_2\lambda_3 + 1)c_1}, \\ \mu_3 &= -\frac{\sqrt{-(4\Lambda^2c_2^2\lambda_3^2 - 2\Lambda b_1^2\mu_1^2 + 4\Lambda c_2\lambda_3 + 1)(2\Lambda c_2^2\lambda_3^2 - b_1^2\mu_1^2 + 2c_2\lambda_3)(2\Lambda c_2\lambda_3 + 1)}}{(4\Lambda^2c_2^2\lambda_3^2 - 2\Lambda b_1^2\mu_1^2 + 4\Lambda c_2\lambda_3 + 1)c_2}. \end{aligned} \tag{3.41}$$

Then, the solution is

$$\begin{aligned} \Sigma_l(z, t) &= \frac{m_l}{h_l} \exp(ic_l \zeta_{l+1}) \operatorname{sech}(b_l \zeta_l), \\ l &= 1, 2, \quad \zeta_k = \lambda_k z + \mu_k(t) + \xi_k, \quad k = 1, 2, 3. \end{aligned} \tag{3.42}$$

Figure 5 depicts the impact of analysis of singular soliton solution where graphs of $\Sigma_l, l = 1, 2$ are given with the following chosen parameters

$$\begin{aligned} \Lambda &= 0.1e - 2, \delta = 1, \lambda_3 = 1, c_1 = 2, c_2 = 3, b_1 = 2, \\ m_1 &= 2, m_2 = 3, \mu_1 = 2, \xi_1 = 1, \xi_2 = 1, \xi_3 = 2.5, \end{aligned} \tag{3.43}$$

$$\Sigma_1 = 8.081071928 \frac{e^{2i(-1.605298328 t - 501.5000000 z + 1)}}{\sqrt{(|2|)^2 + (|3|)^2 \cosh(4t + 12.76579187z + 2)}}, \tag{3.44}$$

$$\begin{aligned} \Lambda = 0.1e - 2, \delta = 1, \lambda_3 = 1, c_1 = 2, c_2 = 3, b_1 = 2, \\ m_1 = 2, m_2 = 3, \mu_1 = 2, \xi_1 = 1, \xi_2 = 1, \xi_3 = 2.5, \end{aligned} \tag{3.45}$$

$$\Sigma_2 = 12.12160789 \frac{e^{3i(-1.070198885 t + z + 2.5)}}{\sqrt{(|2|)^2 + (|3|)^2 \cosh(4t + 12.76579187z + 2)}}, \tag{3.46}$$

in Eq. (3.42). We investigate the dynamics of general bright solitons received from the Hirota bilinear technique, which is presented in Fig. 6. From the figure, it is apparent that the bright solitons exhibit a stable propagation in both components of CNLH system as shown in Figs. 6.

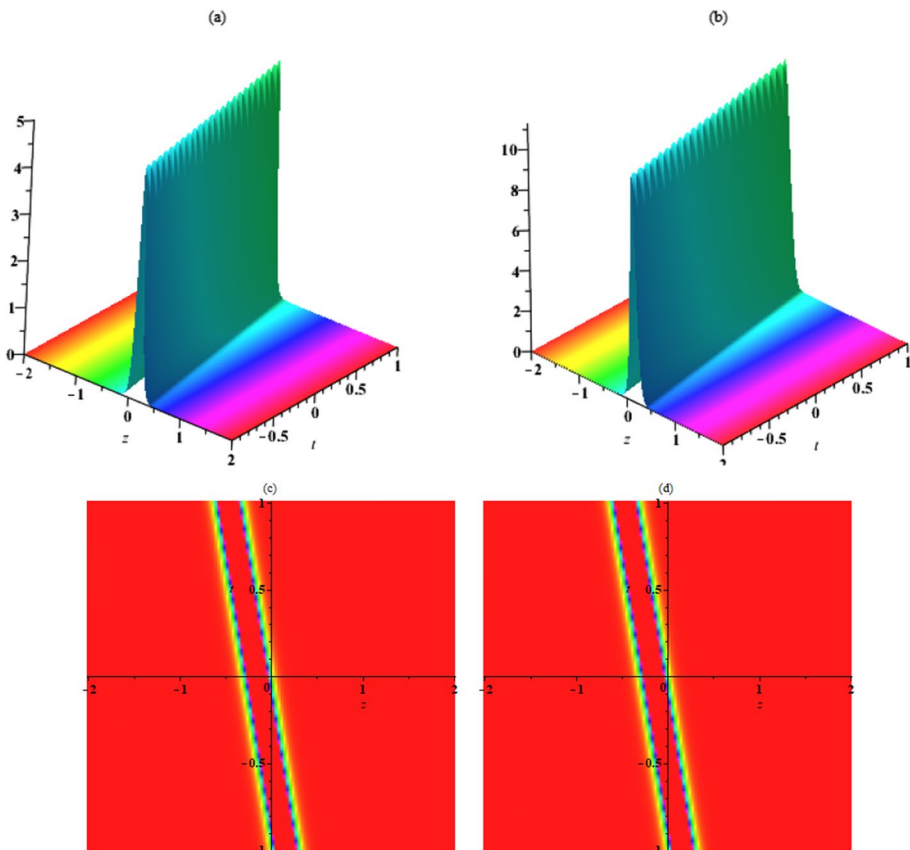


Fig. 6 Plot of soliton solution (3.42) ($|\Sigma_1|^2$) such as left graphs $|\Sigma_1|^2$ and right graphs $|\Sigma_2|^2$

3.3.3 Set III solutions

$$\Sigma_1 = \frac{m_1 e^{ic_1 \left(\frac{\mu_3 c_2}{c_1} - 1/2 \frac{z}{c_1 \Lambda} + \xi_2 \right)} \sqrt{2} \sqrt{\frac{2 \Lambda c_2^2 \mu_3^2 - 1}{\Lambda b_1^2}} b_1}{2 \sqrt{\delta \left((|m_1|)^2 + (|m_2|)^2 \right)} \cosh \left(b_1 \left(1/2 \frac{z \sqrt{2 \Lambda c_2^2 \mu_3^2 - 1}}{b_1 \Lambda} + \xi_1 \right) \right)}, \tag{3.47}$$

$$\Sigma_2 = \frac{m_2 e^{ic_2 \left(\mu_3 - 1/2 \frac{z}{c_2 \Lambda} + \xi_3 \right)} \sqrt{2} \sqrt{\frac{2 \Lambda c_2^2 \mu_3^2 - 1}{\Lambda b_1^2}} b_1}{2 \sqrt{\delta \left((|m_1|)^2 + (|m_2|)^2 \right)} \cosh \left(b_1 \left(1/2 \frac{z \sqrt{2 \Lambda c_2^2 \mu_3^2 - 1}}{b_1 \Lambda} + \xi_1 \right) \right)}, \tag{3.48}$$

such that $\Lambda (b_1)^2 (2 \Lambda c_2^2 \mu_3^2 - 1) > 0$.

3.4 Periodic solutions

Supposing periodic wave solutions as the below function

$$\begin{aligned} f(z, t) &= h_1 \cos(b_1 \zeta_1), \quad g_l(z, t) = m_l \exp(ic_l \zeta_{l+1}), \quad l = 1, 2, \\ \zeta_l &= \lambda_l z + \mu_l(t) + \xi_l, \quad l = 1, 2, 3. \end{aligned} \tag{3.49}$$

By putting $\Sigma_l = g_l(z, t)/f(z, t)$, $l = 1, 2$ Eq. (2.15) and using relations (2.16) and taking the coefficients of the nonlinear expressions to zero, yield a system of algebraic equations including below:

$$\begin{aligned} 2 \Lambda b_1^2 \lambda_1^2 + 2 \Lambda c_1^2 \lambda_2^2 + b_1^2 \mu_1^2 + c_1^2 \mu_2^2 + 2 c_1 \lambda_2 &= 0, \\ -4 i \Lambda c_1 \lambda_2 b_1 \lambda_1 - 2 ic_1 \mu_2 b_1 \mu_1 - 2 ib_1 \lambda_1 &= 0, \\ 2 \Lambda b_1^2 \lambda_1^2 + 2 \Lambda c_2^2 \lambda_3^2 + b_1^2 \mu_1^2 + c_2^2 \mu_3^2 + 2 c_2 \lambda_3 &= 0, \\ -4 i \Lambda c_2 \lambda_3 b_1 \lambda_1 - 2 ic_2 \mu_3 b_1 \mu_1 - 2 ib_1 \lambda_1 &= 0. \end{aligned}$$

Also, by solving $-2 \Lambda b_1^2 h_1^2 \lambda_1^2 - h_1^2 b_1^2 \mu_1^2 - (|m_1|)^2 \delta - (|m_2|)^2 \delta = 0$ we can get to the amplitude of solitary wave as below

$$h_1 = \pm \frac{\sqrt{(2 \Lambda \lambda_1^2 + \mu_1^2) \delta \left((|m_1|)^2 + (|m_2|)^2 \right)}}{(2 \Lambda \lambda_1^2 + \mu_1^2) b_1}. \tag{3.50}$$

Therefore, the form of solutions is as below

$$\Sigma_l = \pm \frac{\sqrt{-(2 \Lambda \lambda_1^2 + \mu_1^2) \delta \left((|m_1|)^2 + (|m_2|)^2 \right)}}{(2 \Lambda \lambda_1^2 + \mu_1^2) b_1} \exp(ic_l \zeta_{l+1}) \sec(b_1 \zeta_1), \quad l = 1, 2. \tag{3.51}$$

By solving the above equations get the following results:

3.4.1 Set I solutions

$$\begin{aligned} \lambda_1 &= \frac{\sqrt{-(4\Lambda^2 c_2^2 \lambda_3^2 + 2\Lambda b_1^2 \mu_1^2 + 4\Lambda c_2 \lambda_3 + 1)(2\Lambda c_2^2 \lambda_3^2 + b_1^2 \mu_1^2 + 2c_2 \lambda_3)} \mu_1}{4\Lambda^2 c_2^2 \lambda_3^2 + 2\Lambda b_1^2 \mu_1^2 + 4\Lambda c_2 \lambda_3 + 1}, \\ \lambda_2 &= \frac{c_2 \lambda_3}{c_1}, \quad \mu_2 = -\frac{\sqrt{-(4\Lambda^2 c_2^2 \lambda_3^2 + 2\Lambda b_1^2 \mu_1^2 + 4\Lambda c_2 \lambda_3 + 1)(2\Lambda c_2^2 \lambda_3^2 + b_1^2 \mu_1^2 + 2c_2 \lambda_3)} (2\Lambda c_2 \lambda_3 + 1)}{(4\Lambda^2 c_2^2 \lambda_3^2 + 2\Lambda b_1^2 \mu_1^2 + 4\Lambda c_2 \lambda_3 + 1)c_1}, \\ \mu_3 &= -\frac{\sqrt{-(4\Lambda^2 c_2^2 \lambda_3^2 + 2\Lambda b_1^2 \mu_1^2 + 4\Lambda c_2 \lambda_3 + 1)(2\Lambda c_2^2 \lambda_3^2 + b_1^2 \mu_1^2 + 2c_2 \lambda_3)} (2\Lambda c_2 \lambda_3 + 1)}{(4\Lambda^2 c_2^2 \lambda_3^2 + 2\Lambda b_1^2 \mu_1^2 + 4\Lambda c_2 \lambda_3 + 1)c_2}. \end{aligned} \tag{3.52}$$

Then, the solution is

$$\begin{aligned} \Sigma_l(z, t) &= \frac{m_l}{h_1} \exp(ic_l \zeta_{l+1}) \operatorname{sec}(b_1 \zeta_l), \\ l &= 1, 2, \quad \zeta_k = \lambda_k z + \mu_k(t) + \xi_k, \quad k = 1, 2, 3. \end{aligned} \tag{3.53}$$

Figure 7 depicts the impact of analysis periodic wave solution where graphs of $\Sigma_l, l = 1, 2$ are given with the following chosen parameters

$$\begin{aligned} \Lambda &= 0.1e - 2, \delta = -1, \lambda_3 = 1, c_1 = 2, c_2 = 3, b_1 = 1, \\ m_1 &= 2, m_2 = 3, \mu_1 = 2, \xi_1 = 1, \xi_2 = 1, \xi_3 = 2.5, \end{aligned} \tag{3.54}$$

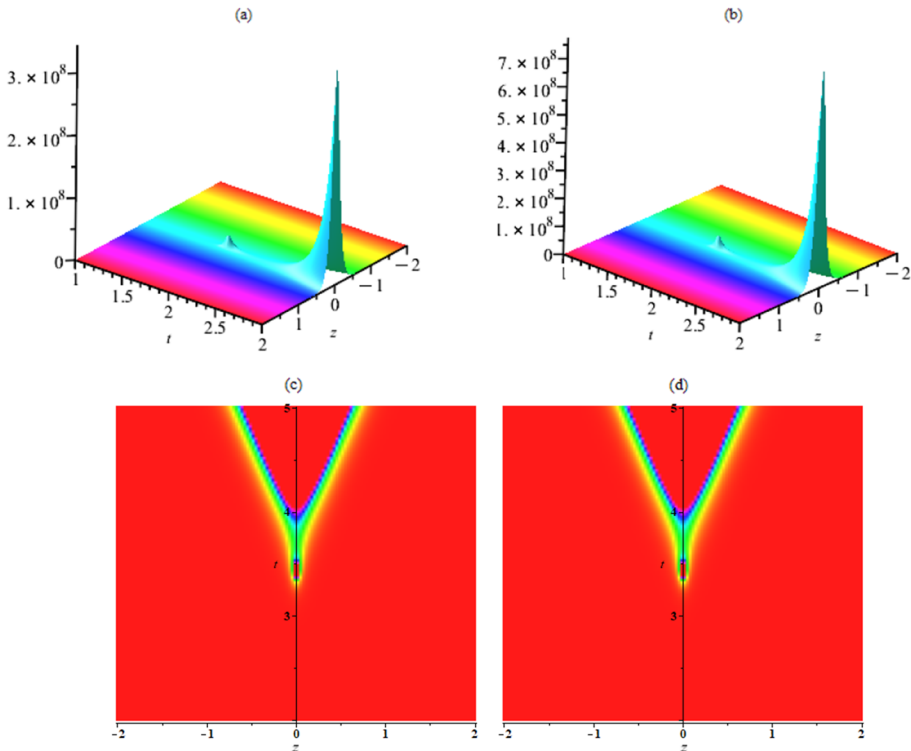


Fig. 7 Plot of periodic wave solution (3.53) ($|\Sigma_l|^2$) such as left graphs $|\Sigma_1|^2$ and right graphs $|\Sigma_2|^2$

$$\Sigma_1 = 3.960520280 \frac{e^{2i(-1.576343096it+3/2z+1)}}{\sqrt{(|2|)^2 + (|3|)^2 \cos(2t + 6.267765789iz + 1)}}, \tag{3.55}$$

$$\begin{aligned} \Lambda = 0.1e - 2, \delta = -1, \lambda_3 = 1, c_1 = 2, c_2 = 3, b_1 = 1, \\ m_1 = 2, m_2 = 3, \mu_1 = 2, \xi_1 = 1, \xi_2 = 1, \xi_3 = 2.5, \end{aligned} \tag{3.56}$$

$$\Sigma_2 = 5.940780420 \frac{e^{3i(-1.050895397it+z+2.5)}}{\sqrt{(|2|)^2 + (|3|)^2 \cos(2t + 6.267765789iz + 1)}}, \tag{3.57}$$

in Eq. (3.53). We investigate the dynamics of general periodic wave received from the Hirota bilinear technique, which is presented in Fig. 7. From the figure, it is apparent that the solitons exhibit a stable propagation in both components of CNLH system as shown in Figs. 7.

3.4.2 Set II solutions

$$\begin{aligned} \lambda_1 &= \frac{\sqrt{-(4\Lambda^2c_2^2\lambda_3^2 + 2\Lambda b_1^2\mu_1^2 + 4\Lambda c_2\lambda_3 + 1)(2\Lambda c_2^2\lambda_3^2 + b_1^2\mu_1^2 + 2c_2\lambda_3)\mu_1}}{4\Lambda^2c_2^2\lambda_3^2 + 2\Lambda b_1^2\mu_1^2 + 4\Lambda c_2\lambda_3 + 1}, \\ \lambda_2 &= \frac{c_2\lambda_3}{c_1}, \mu_2 = -\frac{\sqrt{-(4\Lambda^2c_2^2\lambda_3^2 + 2\Lambda b_1^2\mu_1^2 + 4\Lambda c_2\lambda_3 + 1)(2\Lambda c_2^2\lambda_3^2 + b_1^2\mu_1^2 + 2c_2\lambda_3)}(2\Lambda c_2\lambda_3 + 1)}{(4\Lambda^2c_2^2\lambda_3^2 + 2\Lambda b_1^2\mu_1^2 + 4\Lambda c_2\lambda_3 + 1)c_1}, \\ \mu_3 &= -\frac{\sqrt{-(4\Lambda^2c_2^2\lambda_3^2 + 2\Lambda b_1^2\mu_1^2 + 4\Lambda c_2\lambda_3 + 1)(2\Lambda c_2^2\lambda_3^2 + b_1^2\mu_1^2 + 2c_2\lambda_3)}(2\Lambda c_2\lambda_3 + 1)}{(4\Lambda^2c_2^2\lambda_3^2 + 2\Lambda b_1^2\mu_1^2 + 4\Lambda c_2\lambda_3 + 1)c_2}. \end{aligned} \tag{3.58}$$

Then, the solution is

$$\begin{aligned} \Sigma_l(z, t) &= \frac{m_l}{h_1} \exp(ic_l \zeta_{l+1}) \operatorname{sec}(b_1 \zeta_1), \\ l = 1, 2, \zeta_k &= \lambda_k z + \mu_k(t) + \xi_k, \quad k = 1, 2, 3. \end{aligned} \tag{3.59}$$

Figure 8 depicts the impact of analysis periodic wave solution where graphs of $\Sigma_l, l = 1, 2$ are given with the following parameters

$$\begin{aligned} \Lambda = 0.1e - 2, \delta = -1, \lambda_3 = 1, c_1 = 2, c_2 = 3, b_1 = 1, \\ m_1 = 2, m_2 = 3, \mu_1 = 2, \xi_1 = 1, \xi_2 = 1, \xi_3 = 2.5, \end{aligned} \tag{3.60}$$

$$\Sigma_1 = 3.960520280 \frac{e^{2i(-1.576343096it-501.5000000z+1)}}{\sqrt{(|2|)^2 + (|3|)^2 \cos(2t + 6.267765789iz + 1)}}, \tag{3.61}$$

$$\begin{aligned} \Lambda = 0.1e - 2, \delta = -1, \lambda_3 = 1, c_1 = 2, c_2 = 3, b_1 = 1, \\ m_1 = 2, m_2 = 3, \mu_1 = 2, \xi_1 = 1, \xi_2 = 1, \xi_3 = 2.5, \end{aligned} \tag{3.62}$$

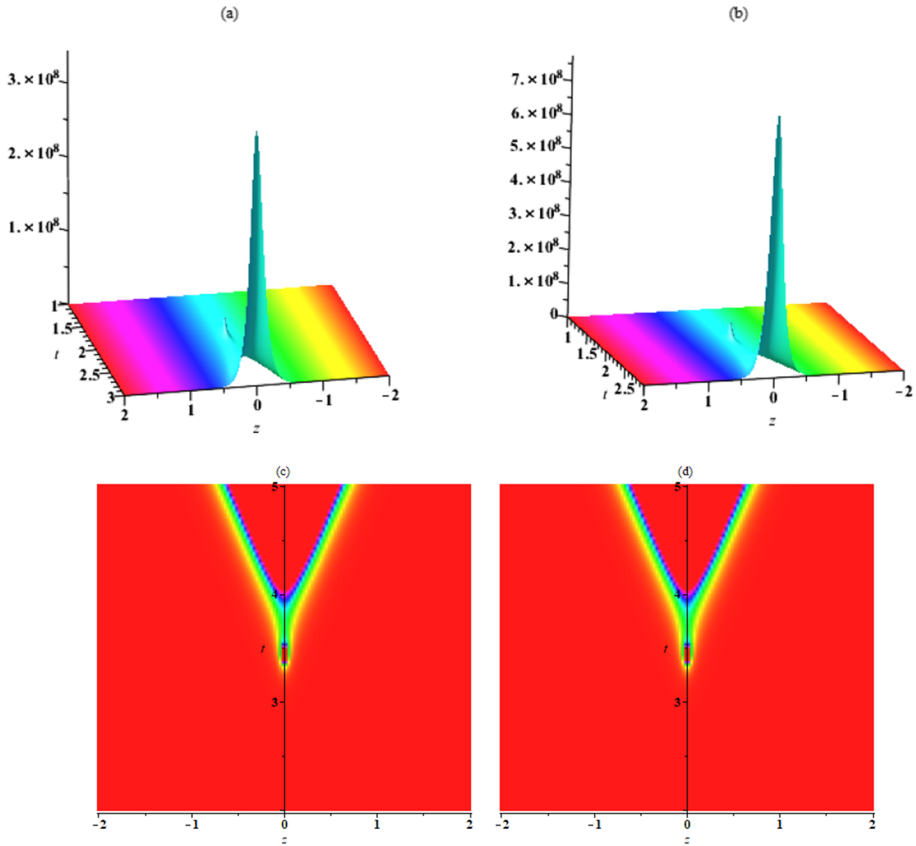


Fig. 8 Plot of soliton solution (3.59) ($|\Sigma_1|^2$) such as left graphs $|\Sigma_1|^2$ and right graphs $|\Sigma_2|^2$

$$\Sigma_2 = 5.940780420 \frac{e^{3i(-1.050895397it+z+2.5)}}{\sqrt{(|2|^2 + |3|^2) \cos(2t + 6.267765789iz + 1)}}, \tag{3.63}$$

in Eq. (3.59). We investigate the dynamics of general periodic wave received from the Hirota bilinear technique, which is presented in Fig. 8. From the figure, it is apparent that the solitons exhibit a stable propagation in both components of CNLH system as shown in Figs. 8.

3.4.3 Set III solutions

$$\Sigma_1 = \frac{m_1 e^{i c_1 \left(-\frac{t \mu_3 c_2}{c_1} - 1/2 \frac{z}{\Lambda c_1} + \xi_2 \right)} \sqrt{2} \sqrt{\frac{-2 \Lambda c_2^2 \mu_3^2 + 1}{\Lambda b_1^2}} b_1}{2 \sqrt{-\delta \left((|m_1|^2 + |m_2|^2) \right)} \cos \left(b_1 \left(1/2 \frac{z \sqrt{-2 \Lambda c_2^2 \mu_3^2 + 1}}{b_1 \Lambda} + \xi_1 \right) \right)}, \tag{3.64}$$

$$\Sigma_2 = \frac{m_2 e^{ic_2 \left(t\mu_3 - 1/2 \frac{z}{\Lambda c_2} + \xi_3 \right)} \sqrt{2} \sqrt{\frac{-2 \Lambda c_2^2 \mu_3^2 + 1}{\Lambda b_1^2}} b_1}{2 \sqrt{-\delta \left((|m_1|)^2 + (|m_2|)^2 \right)} \cos \left(b_1 \left(1/2 \frac{z \sqrt{-2 \Lambda c_2^2 \mu_3^2 + 1}}{b_1 \Lambda} + \xi_1 \right) \right)}, \tag{3.65}$$

such that $(2 \Lambda c_2^2 \mu_3^2 - 1) < 0$.

3.5 Singular form of solutions

Supposing singular form of solution as the below function

$$\begin{aligned} f(z, t) &= h_1 \sin(b_1 \zeta_1), \quad g_l(z, t) = m_l \exp(ic_l \zeta_{l+1}), \quad l = 1, 2, \\ \zeta_l &= \lambda_l z + \mu_l(t) + \xi_l, \quad l = 1, 2, 3. \end{aligned} \tag{3.66}$$

By putting $\Sigma_l = g_l(z, t)/f(z, t)$, $l = 1, 2$ Eq. (2.15) and using relations (2.16) and taking the coefficients of the nonlinear expressions to zero, yield a system of algebraic equations including below:

$$\begin{aligned} 4i\Lambda c_1 \lambda_2 b_1 \lambda_1 + 2ic_1 \mu_2 b_1 \mu_1 + 2ib_1 \lambda_1 &= 0, \\ 2\Lambda b_1^2 \lambda_1^2 + 2\Lambda c_1^2 \lambda_2^2 + b_1^2 \mu_1^2 + c_1^2 \mu_2^2 + 2c_1 \lambda_2 &= 0, \\ 4i\Lambda c_2 \lambda_3 b_1 \lambda_1 + 2ic_2 \mu_3 b_1 \mu_1 + 2ib_1 \lambda_1 &= 0, \\ 2\Lambda b_1^2 \lambda_1^2 + 2\Lambda c_2^2 \lambda_3^2 + b_1^2 \mu_1^2 + c_2^2 \mu_3^2 + 2c_2 \lambda_3 &= 0. \end{aligned}$$

Also, by solving $-2\Lambda b_1^2 h_1^2 \lambda_1^2 - h_1^2 b_1^2 \mu_1^2 - \delta (|m_1|)^2 - \delta (|m_2|)^2 = 0$ we can get to the amplitude of solitary wave as below

$$h_1 = \frac{\sqrt{-(2\Lambda \lambda_1^2 + \mu_1^2) \delta \left((|m_1|)^2 + (|m_2|)^2 \right)}}{(2\Lambda \lambda_1^2 + \mu_1^2) b_1}. \tag{3.67}$$

Therefore, the form of solutions is as below

$$\Sigma_l = \pm \frac{\sqrt{-(2\Lambda \lambda_1^2 + \mu_1^2) \delta \left((|m_1|)^2 + (|m_2|)^2 \right)}}{(2\Lambda \lambda_1^2 + \mu_1^2) b_1} \exp(ic_l \zeta_{l+1}) \operatorname{csc}(b_1 \zeta_1), \quad l = 1, 2. \tag{3.68}$$

By solving the above equations get the following results:

3.5.1 Set I solutions

$$\begin{aligned} h_1 &= 1/2 \frac{\sqrt{-2\Lambda \lambda_1^2 \delta \left((|m_1|)^2 + (|m_2|)^2 \right)}}{\Lambda \lambda_1^2 b_1}, \quad c_1 = 1/2 \frac{\sqrt{-2\Lambda (4\Lambda^2 b_1^2 \lambda_1^2 - 1)}}{\Lambda \mu_2}, \quad \mu_1 = 0, \\ c_2 &= 1/2 \frac{\sqrt{-2\Lambda (4\Lambda^2 b_1^2 \lambda_1^2 - 1)}}{\Lambda \mu_3}, \quad \lambda_2 = -\frac{\mu_2}{\sqrt{-2\Lambda (4\Lambda^2 b_1^2 \lambda_1^2 - 1)}}, \quad \lambda_3 = -\frac{\mu_3}{\sqrt{-2\Lambda (4\Lambda^2 b_1^2 \lambda_1^2 - 1)}}. \end{aligned} \tag{3.69}$$

Then, the solution is

$$\Sigma_l(z, t) = \frac{m_l}{h_1} \exp(ic_l \zeta_{l+1}) \operatorname{csc}(b_1 \zeta_1), \tag{3.70}$$

$$l = 1, 2, \quad \zeta_k = \lambda_k z + \mu_k(t) + \xi_k, \quad k = 1, 2, 3.$$

Figure 9 depicts the impact of analysis singular wave solution where graphs of $\Sigma_l, l = 1, 2$ are given with the following parameters

$$\begin{aligned} \Lambda = 0.1e - 2, \delta = -1, \lambda_1 = 2, b_1 = 1, m_1 = 2, m_2 = 3, \\ \mu_2 = 2, \mu_3 = 3, \xi_1 = 1, \xi_2 = 1, \xi_3 = 2.5, \end{aligned} \tag{3.71}$$

$$\Sigma_1 = 0.016 \frac{e^{11.18025044 i(2t - 44.72171732z + 1)}}{\sqrt{0.008 (|2|)^2 + 0.008 (|3|)^2 \sin(2z + 1)}}, \tag{3.72}$$

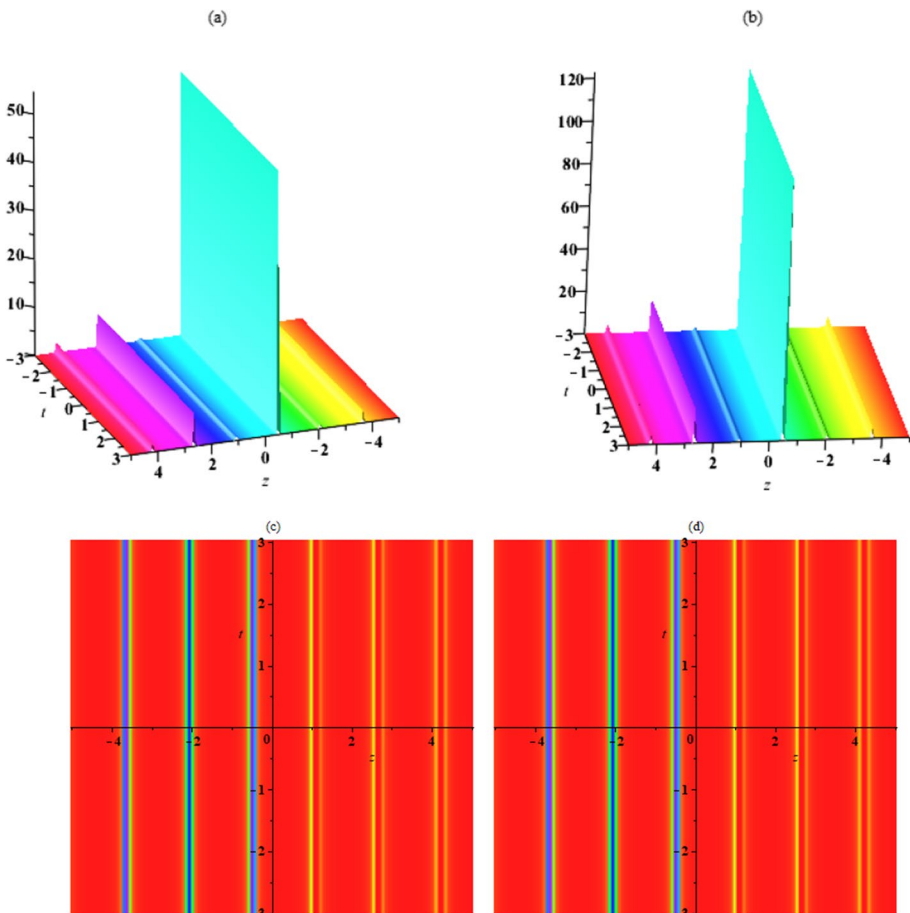


Fig. 9 Plot of singular solution (3.69) ($|\Sigma_l|^2$) such as left graphs $|\Sigma_1|^2$ and right graphs $|\Sigma_2|^2$

$$\Lambda = 0.1e - 2, \delta = -1, \lambda_1 = 2, b_1 = 1, m_1 = 2, m_2 = 3, \mu_2 = 2, \mu_3 = 3, \xi_1 = 1, \xi_2 = 1, \xi_3 = 2.5, \tag{3.73}$$

$$\Sigma_2 = 0.024 \frac{e^{7.453500295 i(3 t - 67.08257598 z + 2.5)}}{\sqrt{0.008 (|2|)^2 + 0.008 (|3|)^2 \sin(2 z + 1)}}, \tag{3.74}$$

in Eq. (3.69). We investigate the dynamics of general singular soliton received from the Hirota bilinear technique, which is presented in Fig. 9. From the figure, it is apparent that the solitons exhibit a stable propagation in both components of CNLH system as shown in Figs. 9.

3.5.2 Set II solutions

$$\begin{aligned} \lambda_1 &= \frac{\sqrt{-(4 \Lambda^2 c_2^2 \lambda_3^2 + 2 \Lambda b_1^2 \mu_1^2 + 4 \Lambda c_2 \lambda_3 + 1)(2 \Lambda c_2^2 \lambda_3^2 + b_1^2 \mu_1^2 + 2 c_2 \lambda_3) \mu_1}}{4 \Lambda^2 c_2^2 \lambda_3^2 + 2 \Lambda b_1^2 \mu_1^2 + 4 \Lambda c_2 \lambda_3 + 1}, \\ \lambda_2 &= \frac{c_2 \lambda_3}{c_1}, \quad \mu_2 = -\frac{\sqrt{-(4 \Lambda^2 c_2^2 \lambda_3^2 + 2 \Lambda b_1^2 \mu_1^2 + 4 \Lambda c_2 \lambda_3 + 1)(2 \Lambda c_2^2 \lambda_3^2 + b_1^2 \mu_1^2 + 2 c_2 \lambda_3)(2 \Lambda c_2 \lambda_3 + 1)}}{(4 \Lambda^2 c_2^2 \lambda_3^2 + 2 \Lambda b_1^2 \mu_1^2 + 4 \Lambda c_2 \lambda_3 + 1) c_1}, \\ \mu_3 &= -\frac{\sqrt{-(4 \Lambda^2 c_2^2 \lambda_3^2 + 2 \Lambda b_1^2 \mu_1^2 + 4 \Lambda c_2 \lambda_3 + 1)(2 \Lambda c_2^2 \lambda_3^2 + b_1^2 \mu_1^2 + 2 c_2 \lambda_3)(2 \Lambda c_2 \lambda_3 + 1)}}{(4 \Lambda^2 c_2^2 \lambda_3^2 + 2 \Lambda b_1^2 \mu_1^2 + 4 \Lambda c_2 \lambda_3 + 1) c_2}, \\ h_1 &= \frac{\sqrt{-\delta \left((|m_1|)^2 + (|m_2|)^2 \right)}}{\sqrt{-2 \frac{\Lambda(2 \Lambda c_2^2 \lambda_3^2 + b_1^2 \mu_1^2 + 2 c_2 \lambda_3) \mu_1^2}{4 \Lambda^2 c_2^2 \lambda_3^2 + 2 \Lambda b_1^2 \mu_1^2 + 4 \Lambda c_2 \lambda_3 + 1} + \mu_1^2 b_1}}. \end{aligned} \tag{3.75}$$

Then, the solution is

$$\begin{aligned} \Sigma_l(z, t) &= \frac{m_l}{h_1} \exp(i c_l \zeta_{l+1}) \operatorname{csc}(b_1 \zeta_1), \\ l &= 1, 2, \quad \zeta_k = \lambda_k z + \mu_k(t) + \xi_k, \quad k = 1, 2, 3. \end{aligned} \tag{3.76}$$

Figure 10 depicts the impact of analysis treatment of singular solution where graphs of $\Sigma_l, l = 1, 2$ are given with the following values

$$\Lambda = 0.1e - 2, \delta = -1, \lambda_3 = 2, c_1 = 2, c_2 = 3, b_1 = 1, m_1 = 2, m_2 = 3, \mu_1 = 2, \xi_1 = 1, \xi_2 = 1, \xi_3 = 1, \tag{3.77}$$

$$\Sigma_1 = 7.784458700 \frac{e^{2 i(-2.608708939 i t + 3 z + 1)}}{\sqrt{(|2|)^2 + (|3|)^2 \sin(4 t + 20.62220506 i z + 2)}}, \tag{3.78}$$

$$\Lambda = 0.1e - 2, \delta = -1, \lambda_3 = 2, c_1 = 2, c_2 = 3, b_1 = 1, m_1 = 2, m_2 = 3, \mu_1 = 2, \xi_1 = 1, \xi_2 = 1, \xi_3 = 1, \tag{3.79}$$

$$\Sigma_2 = 5.905832211 \frac{e^{3 i(-1.331141041 i t + 2 z + 1)}}{\sqrt{(|2|)^2 + (|3|)^2 \sin(2 t + 7.892140556 i z + 1)}}, \tag{3.80}$$

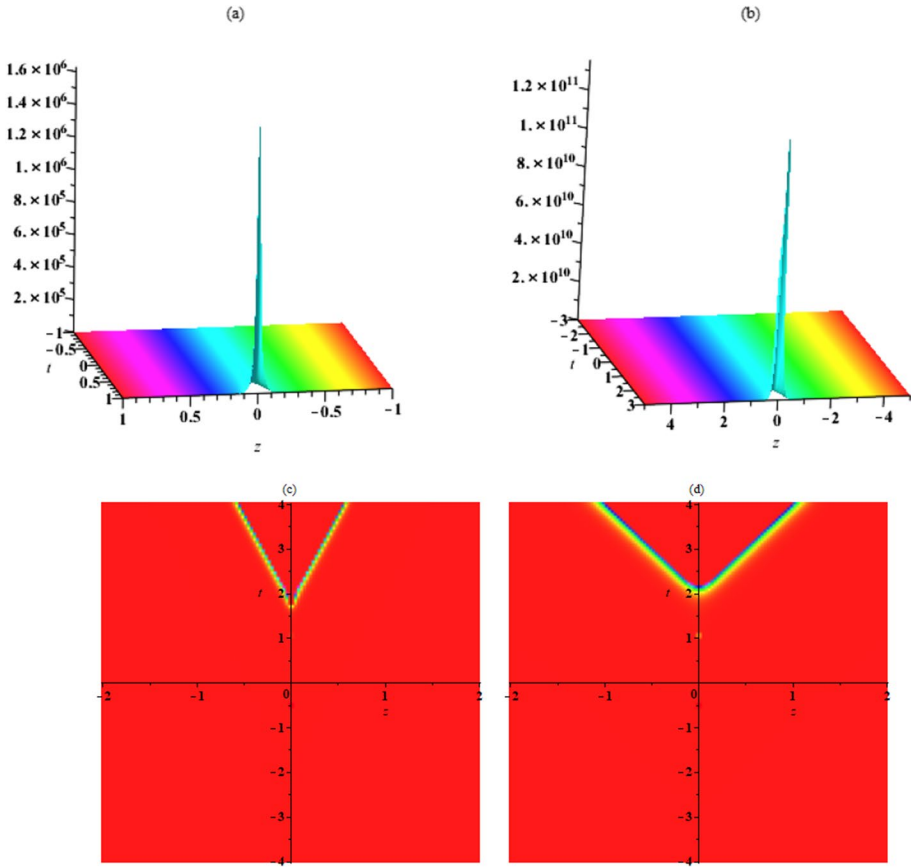


Fig. 10 Plot of singular solution (3.76) ($|\Sigma_1|^2$) such as left graphs $|\Sigma_1|^2$ and right graphs $|\Sigma_2|^2$

in Eq. (3.76). We investigate the dynamics of general singular solution received from the Hirota bilinear technique, which is presented in Fig. 10. From the figure, it is apparent that the solitons exhibit a stable propagation in both components of CNLH system as shown in Figs. 10.

3.5.3 Set III solutions

$$\Sigma_1 = \frac{m_1 e^{ic_1 \left(\frac{t \sqrt{-(4\Lambda^2 c_2^2 \lambda_3^2 + 2\Lambda b_1^2 \mu_1^2 + 4\Lambda c_2 \lambda_3 + 1)} (2\Lambda c_2^2 \lambda_3^2 + b_1^2 \mu_1^2 + 2c_2 \lambda_3) (2\Lambda c_2 \lambda_3 + 1) - \frac{z(\Lambda c_2 \lambda_3 + 1) + \xi_2}{\Lambda c_1}}}{(4\Lambda^2 c_2^2 \lambda_3^2 + 2\Lambda b_1^2 \mu_1^2 + 4\Lambda c_2 \lambda_3 + 1) c_1} \right)}}{h_1 \sin \left(b_1 \left(t \mu_1 + \frac{z \sqrt{-(4\Lambda^2 c_2^2 \lambda_3^2 + 2\Lambda b_1^2 \mu_1^2 + 4\Lambda c_2 \lambda_3 + 1)} (2\Lambda c_2^2 \lambda_3^2 + b_1^2 \mu_1^2 + 2c_2 \lambda_3) \mu_1}{4\Lambda^2 c_2^2 \lambda_3^2 + 2\Lambda b_1^2 \mu_1^2 + 4\Lambda c_2 \lambda_3 + 1} + \xi_1 \right) \right)}, \tag{3.81}$$

$$\Sigma_2 = \frac{i c_2 \left(-\frac{\sqrt{-\left(4 \Lambda^2 c_2^2 \lambda_3^2+2 \Lambda b_1^2 \mu_1^2+4 \Lambda c_2 \lambda_3+1\right)\left(2 \Lambda c_2^2 \lambda_3^2+b_1^2 \mu_1^2+2 c_2 \lambda_3\right)}{\left(4 \Lambda^2 c_2^2 \lambda_3^2+2 \Lambda b_1^2 \mu_1^2+4 \Lambda c_2 \lambda_3+1\right) c_2}+z \lambda_3+\xi_3\right)}{h_1 \sin \left(b_1 \left(t \mu_1 + \frac{z \sqrt{-\left(4 \Lambda^2 c_2^2 \lambda_3^2+2 \Lambda b_1^2 \mu_1^2+4 \Lambda c_2 \lambda_3+1\right)\left(2 \Lambda c_2^2 \lambda_3^2+b_1^2 \mu_1^2+2 c_2 \lambda_3\right)} \mu_1}{4 \Lambda^2 c_2^2 \lambda_3^2+2 \Lambda b_1^2 \mu_1^2+4 \Lambda c_2 \lambda_3+1} + \xi_1 \right) \right)}, \tag{3.82}$$

such that $h_1 = \frac{\sqrt{-\delta \left(\left(|m_1| \right)^2 + \left(|m_2| \right)^2 \right) \left(4 \Lambda^2 c_2^2 \lambda_3^2 + 2 \Lambda b_1^2 \mu_1^2 + 4 \Lambda c_2 \lambda_3 + 1 \right)}}{\mu_1 b_1}$.

4 Physical interpretation of solutions

The (1+1)-dimensional coupled nonlinear Helmholtz systems has been examined by using Hirota’s bilinear scheme. Three exact solutions to soliton, bright soliton, singular soliton, periodic wave and singular form of solutions have been obtained for Eq. (1.1). All the solutions depicted solitary wave solutions in the form of rational wave solutions. The physical phenomena of the solution graphs of (1+1)-dimensional coupled nonlinear Helmholtz systems is given as follows: Fig. 1 represents the singular soliton behaviour of Eqs. (3.5) and (3.7) for the parametric values $\Lambda = 0.1e - 2, \delta = 1, \lambda_1 = 1, \lambda_2 = 1, \lambda_4 = 1, c_1 = 1, c_2 = 2, b_1 = 1, b_2 = 2.5, h_1 = 1, \mu_1 = 1, m_1 = 2, \mu_2 = 2, \mu_4 = 3, \xi_1 = 1, \xi_2 = 1, \xi_3 = 2.5$. However, Fig. 2 depicts the singular soliton behaviour of Eqs. (3.11) and (3.13) for the parametric values $\Lambda = 0.1e - 2, \delta = 1, \lambda_1 = 1, \lambda_2 = 1, \lambda_4 = 1, c_1 = 1, c_2 = 2, b_1 = 1, b_2 = 2.5, h_1 = 1, \mu_1 = 1, m_1 = 2, \mu_2 = 2, \mu_4 = 3, \xi_1 = 1, \xi_2 = 1, \xi_3 = 2.5$. Figure 3 represents the soliton behaviour of Eqs. (3.21) and (3.23) for the parametric values $\Lambda = 0.1e - 2, \delta = -1, \lambda_3 = 1, c_1 = 1, c_2 = 2, b_1 = \frac{2}{3}, m_1 = 2, \mu_2 = 2, \mu_1 = 1, \xi_1 = 1, \xi_2 = 1, \xi_3 = 2.5$. Figure 4 shows the soliton behaviour of Eqs. (3.27) and (3.29) for the parametric values $\Lambda = 0.1e - 2, \delta = -1, \lambda_3 = 1, c_1 = 1, c_2 = 2, b_1 = \frac{4}{3}, m_1 = 2, \mu_2 = 2, \mu_1 = 1, \xi_1 = 1, \xi_2 = 1, \xi_3 = 2.5$. While, the bright soliton behaviour of Eqs. (3.38) and (3.40) for the parametric values $\Lambda = 0.1e - 2, \delta = 1, \lambda_3 = 1, c_1 = 2, c_2 = 3, b_1 = \frac{5}{4}, m_1 = 2, m_2 = 3, \mu_1 = 2, \xi_1 = 1, \xi_2 = 1, \xi_3 = 2.5$ has been seen in Fig. 5. And the bright soliton behaviour of Eqs. (3.44) and (3.46) for the parametric values $\Lambda = 0.1e - 2, \delta = 1, \lambda_3 = 1, c_1 = 2, c_2 = 3, b_1 = 2, m_1 = 2, m_2 = 3, \mu_1 = 2, \xi_1 = 1, \xi_2 = 1, \xi_3 = 2.5$ has been seen in Fig. 6. Also, the periodic wave behaviour of Eqs. (3.55) and (3.57) for the parametric values $\Lambda = 0.1e - 2, \delta = -1, \lambda_3 = 1, c_1 = 2, c_2 = 3, b_1 = 1, m_1 = 2, m_2 = 3, \mu_1 = 2, \xi_1 = 1, \xi_2 = 1, \xi_3 = 2.5$ has been seen in Fig. 7. Moreover, the periodic wave behaviour of Eqs. (3.61) and (3.63) for the parametric values $\Lambda = 0.1e - 2, \delta = -1, \lambda_3 = 1, c_1 = 2, c_2 = 3, b_1 = 1, m_1 = 2, m_2 = 3, \mu_1 = 2, \xi_1 = 1, \xi_2 = 1, \xi_3 = 2.5$ has been shown in Fig. 8. While, Fig. 9 displays the singular wave behaviour of Eqs. (3.72) and (3.74) for the parametric values $\Lambda = 0.1e - 2, \delta = -1, \lambda_1 = 2, b_1 = 1, m_1 = 2, m_2 = 3, \mu_3 = 3, \xi_1 = 1, \xi_2 = 1, \xi_3 = 2.5$. Finally, the singular wave behaviour of Eqs. (3.78) and (3.80) for the parametric values $\Lambda = 0.1e - 2, \delta = -1, \lambda_3 = 2, c_1 = 2, c_2 = 3, b_1 = 1, m_1 = 2, m_2 = 3, \mu_1 = 2, \xi_1 = 1, \xi_2 = 1, \xi_3 = 1$ has been displayed in Fig. 10.

5 Comparison and novelty

Here, some concrete instances of our research findings and critically evaluate their originality are offered. Plenty of computational and approximate solutions to the issue at hand have been devised utilizing five modern analytical and numerical schemes. These solutions have been presented in a number of various ways employing numerical plots (1-10), displaying phenomena like singular soliton, soliton, bright soliton, periodic wave, and singular wave solutions in three-dimensional and density approaches. When presenting our findings, we compared them to those that had already been published (Christian et al. 2006; Chamorro-Posada and McDonald 2006; Song et al. 2020) to highlight the uniqueness of our findings. It is clear that our results are not consistent with those found in these publications.

6 Conclusion

To conclude, the nonparaxial solitary wave by using the Hirota's bilinear scheme were analytically constructed. We noticed that the systems was non-integrable. The impact of nonparaxiality on the physical parameters such as speed and amplitudes of solitary waves were emphasized. The binary bell polynomials and bilinear transformation to the nonlinear system were studied. In particular, five forms of function solution including soliton, bright soliton, singular soliton, periodic wave and singular form of solutions were studied. To achieve this, an illustrative example of the coupled nonlinear Helmholtz systems was provided to demonstrate the feasibility and reliability of the procedure used in this study. The effect of the free parameters on the behavior of acquired figures to a few obtained solutions for two nonlinear rational exact cases was also discussed. For a better understanding on the resulting dynamics, a categorical discussion and clear graphical demonstration for solitons and periodic wave on both constant and spatially-varying backgrounds were provided. Further, the periodic and hyperbolic solutions with arbitrary spatial backgrounds for the considered model (1.1) through bilinear transformation were obtained. The obtained results will be an important addition along the context of nonlinear wave manipulation in higher-dimensional models due to controllable backgrounds. The present investigation shall also be extended to several other solitonic models towards improved understanding on the dynamical characteristics of respective nonlinear waves

Acknowledgements The researchers would like to acknowledge the Deanship of Scientific Research, Taif University, for funding this work.

Author Contributions The authors contributed equally and significantly in writing this paper. All authors read and approved the final manuscript.

Funding This paper is supported by the guiding project B2019048 of Science and Technology Research Plan of Education Department of Hubei Province: Theoretical research on Stability of Complex Networks.

Data availability Please contact author for data requests.

Declarations

Competing interests: Authors declare they have no competing interests regarding the publication of the article.

References

- Ali, N.H., Mohammed, S.A., Manafian, J.: New explicit soliton and other solutions of the van der Waals model through the ESHGEEM and the IEEM. *J. Mod. Tech. Eng.* **8**(1), 5–18 (2023)
- Alimirzaluo, E., Nadjafikhah, M., Manafian, J.: Some new exact solutions of (3+1)-dimensional Burgers system via Lie symmetry analysis. *Adv. Diff. Eq.* **2021**, 60 (2021)
- Arshad, M., Lu, D., Wang, J.: (N+1)-dimensional fractional reduced differential transform method for fractional order partial differential equations. *Commun. Nonlinear Sci. Num. Simul.* **48**, 509–519 (2017)
- Aslanova, F.: A comparative study of the hardness and force analysis methods used in truss optimization with metaheuristic algorithms and under dynamic loading. *J. Res. Sci. Eng. Tech.* **8**(1), 25–33 (2020)
- Bai, X., Shi, H., Zhang, K., Zhang, X., Wu, Y.: Effect of the fit clearance between ceramic outer ring and steel pedestal on the sound radiation of full ceramic ball bearing system. *J. Sound Vib.* **529**, 116967 (2022)
- Bouchaala, F., Ali, M.Y., Matsushima, J., Bouzidi, Y., Takam Takougang, E.M., Mohamed, A.A., Sultan, A.: Azimuthal investigation of compressional seismic-wave attenuation in a fractured reservoir. *Geophysics* **84**(6), B437–B446 (2019)
- Bouchaala, F., Ali, M.Y., Matsushima, J., Bouzidi, Y., Jouini, M.S., Takougang, E.M., Mohamed, A.A.: Estimation of seismic wave attenuation from 3D seismic data: a case study of OBC data acquired in an offshore oilfield. *Energies* **15**(2), 534 (2022)
- Brown, P., Mazumder, P.: Current progress in mechanically durable water-repellent surfaces: a critical review. *Rev. Adhes. Adhes.* **9**(1), 123–152 (2021)
- Cai, W., Mohammaditab, R., Fathi, G., Wakil, K., Ebadi, A.G., Ghadimi, N.: Optimal bidding and offering strategies of compressed air energy storage: a hybrid robust-stochastic approach. *Renew. Energy* **143**, 1–8 (2019)
- Chamorro-Posada, P., McDonald, G.S.: Spatial Kerr soliton collisions at arbitrary angles. *Phys. Rev. E* **74**, 036609 (2006)
- Chen, L., Huang, H., Tang, P., Yao, D., Yang, H., Ghadimi, N.: Optimal modeling of combined cooling, heating, and power systems using developed African vulture optimization: a case study in watersport complex. *Energy Sources A* **44**, 4296–4317 (2022)
- Christian, J.M., McDonald, G.S., Chamorro-Posada, P.: Helmholtz–Manakov solitons. *Phys. Rev. E* **74**, 066612 (2006)
- Dai, Z., Xie, J., Jiang, M.: A coupled peridynamics-smoothed particle hydrodynamics model for fracture analysis of fluid-structure interactions. *Ocean Eng.* **279**, 114582 (2023)
- Davoodabadi, I., Ramezani, A.A., Mahmoodi-k, M., Ahmadizadeh, P.: Identification of tire forces using Dual Unscented Kalman Filter algorithm. *Nonlinear Dyn.* **78**, 1907–1919 (2014)
- Dawod, L.A., Lakestani, M., Manafian, J.: Breather wave solutions for the (3+1)-D generalized shallow water wave equation with variable coefficients. *Qual. Theo. Dyn. Sys.* **22**, 127 (2023)
- Della Volpe, C., Siboni, S.: From van der Waals equation to acid-base theory of surfaces: a chemical–mathematical journey. *Rev. Adh. Adhes.* **10**(1), 47–97 (2022)
- Du, S., Xie, H., Yin, J., Fang, T., Zhang, S., Sun, Y., Zheng, R.: Competition pathways of energy relaxation of hot electrons through coupling with optical, surface, and acoustic phonons. *J. Phys. Chem. C* **127**(4), 1929–1936 (2023)
- Erfeng, H., Ghadimi, N.: Model identification of proton-exchange membrane fuel cells based on a hybrid convolutional neural network and extreme learning machine optimized by improved honey badger algorithm. *Sustain. Energy Tech. Asses.* **52**, 102005 (2022)
- Ghasemvand, M., Behjat, B., Ebrahimi, S.: Experimental investigation of the effects of adhesive defects on the strength and creep behavior of single-lap adhesive joints at various temperatures. *J. Adhesion* **99**, 1227–1243 (2023)
- Gu, Y., Malmir, S., Manafian, J., Ilhan, O.A., Alizadeh, A., Othman, A.J.: Variety interaction between K -lump and K -kink solutions for the (3+1)-D Burger system by bilinear analysis. *Results Phys.* **43**, 106032 (2022)
- Guo, C., Hu, J., Wu, Y., Čelikovský, S.: Non-singular fixed-time tracking control of uncertain nonlinear pure-feedback systems with practical state constraints. *IEEE Trans. Circuits Syst. I* (2023) <https://doi.org/10.1109/TCSI.2023.3291700>
- Guo, C., Hu, J.: Fixed-time stabilization of high-order uncertain nonlinear systems: output feedback control design and settling time analysis. *J. Syst. Sci. Complexity* (2023). <https://doi.org/10.1007/s11424-023-2370-y>
- Guo, C., Hu, J., Hao, J., Čelikovský, S., Hu, X.: Fixed-time safe tracking control of uncertain high-order nonlinear pure-feedback systems via unified transformation functions. *Kybernetika* **59**(3), 342–364 (2023)

- Han, E., Ghadimi, N.: Model identification of proton-exchange membrane fuel cells based on a hybrid convolutional neural network and extreme learning machine optimized by improved honey badger algorithm. *Sustain Energy Tech. Asses.* **52**, 102005 (2022)
- Hansryd, J., Andrekson, P.A., Westlund, M., Li, J., Hedekvist, P.O.: Fiber-based optical parametric amplifiers and their applications. *IEEE J. Sel. Top. Quant. Elec.* **8**, 506 (2002)
- Jiang, W., Wang, X., Huang, H., Zhang, D., Ghadimi, N.: Optimal economic scheduling of microgrids considering renewable energy sources based on energy hub model using demand response and improved water wave optimization algorithm. *J. Energy Storage* **55**(1), 105311 (2022)
- Jin, H.Y., Wang, Z.: Asymptotic dynamics of the one-dimensional attraction-repulsion Keller–Segel model. *Math. Meth. Appl. Sci.* **38**(3), 444–457 (2015)
- Kivshar, Y., Agrawal, G.: *Optical Solitons: From Fibers to Photonic Crystals*. Elsevier, Amsterdam (2003)
- Ku, T.S., Shih, M.F., Sukhorukov, A.A., Kivshar, Y.S.: Incoherent multi-gap optical solitons in nonlinear photonic lattices. *Phys. Rev. Lett.* **94**, 063904 (2005)
- Lakshmanan, M., Rajasekar, S.: *Nonlinear Dynamics: Integrability, Chaos and Patterns*. Springer, Berlin (2003)
- Li, R., Bu Sinnah, Z.A., Shatouri, Z.M., Manafian, J., Aghdaei, M.F., Kadi, A.: Different forms of optical soliton solutions to the Kudryashov’s quintuple self-phase modulation with dual-form of generalized nonlocal nonlinearity. *Results Phys.* **46**, 106293 (2023)
- Liu, X., Abd Alreda, B., Manafian, J., Eslami, B., Aghdaei, M.F., Abotaleb, M., Kadi, A.: Computational modeling of wave propagation in plasma physics over the Gilson-Pickering equation. *Results Phys.* **50**, 106579 (2023)
- Liu, J.G., Zhou, L., He, Y.: Multiple soliton solutions for the new (2+1)-dimensional Korteweg-de Vries equation by multiple exp-function method. *Appl. Math. Let.* **80**, 71–78 (2018)
- Liu, F.Y., Gao, Y.T., Yu, X., Hu, L., Wu, X.H.: Hybrid solutions for the (2+1)-dimensional variable-coefficient Caudrey–Dodd–Gibbon–Kotera–Sawada equation in fluid mechanics. *Chaos Solitons Fract.* **152**, 111355 (2021)
- Lyu, W., Wang, Z.: Logistic damping effect in chemotaxis models with density-suppressed motility. *Adv. Nonlinear Anal.* **12**(1), 0263 (2023). <https://doi.org/10.1515/anona-2022->
- Ma, W.X.: Bilinear equations, Bell polynomials and linear superposition principle. *J. Phys. Conf. Ser.* **411**, 012021 (2013)
- Madina, B., Gumilyov, L.N.: Determination of the most effective location of environmental hardenings in concrete cooling tower under far-source seismic using linear spectral dynamic analysis results. *J. Res. Sci. Eng. Tech.* **8**(1), 22–24 (2020)
- Mahmoodi-k, M., Davoodabadi, I., Višnjić, V., Afkar, A.: Stress and dynamic analysis of optimized trailer chassis. *Tehnički vjesnik* **21**(3), 599–608 (2014)
- Manafian, J., Lakestani, M.: N-lump and interaction solutions of localized waves to the (2+1)-dimensional variable-coefficient Caudrey–Dodd–Gibbon–Kotera–Sawada equation. *J. Geo. Phys.* **150**, 103598 (2020)
- Manafian, J., Mohammed, S.A., Alizadeh, A., Baskonus, H.M., Gao, W.: Investigating lump and its interaction for the third-order evolution equation arising propagation of long waves over shallow water. *Eur. J. Mech. B/Fluids* **84**, 289–301 (2020)
- Mehrpooaya, M., Ghadimi, N., Marefati, M., Ghorbanian, S.A.: Numerical investigation of a new combined energy system includes parabolic dish solar collector, Stirling engine and thermoelectric device. *Int. J. Energy Res.* **45**(11), 16436–16455 (2021)
- Meng, Q., Ma, Q., Shi, Y.: Adaptive fixed-time stabilization for a class of uncertain nonlinear systems. *IEEE Trans. Automatic Control* (2023). <https://doi.org/10.1109/TAC.2023.3244151>
- Mir, M., Shafieezadeh, M., Heidari, M.A., Ghadimi, N.: Application of hybrid forecast engine based intelligent algorithm and feature selection for wind signal prediction. *Evolv. Sys.* **11**(4), 559–573 (2020)
- Moghadam, R.A., Ebrahimi, S.: Design and analysis of a torsional mode MEMS disk resonator for RF applications. *J. Multidisc. Eng. Sci. Tech.* **8**(7), 14300–14303 (2021)
- Mojtahedi, A., Hokmabady, H., Kouhi, M., Mohammadyzadeh, S.: A novel ANN-RDT approach for damage detection of a composite panel employing contact and non-contact measuring data. *Compos. Struct.* **279**, 114794 (2022)
- Pourghanbar, S., Manafan, J., Ranjbar, M., Aliyeva, A., Gasimov, Y.S.: An efficient alternating direction explicit method for solving a nonlinear partial differential equation. *Math. Probl. Eng.* **2020**, 9647416 (2020)
- Ren, B., Ma, W.X., Yu, J.: Rational solutions and their interaction solutions of the (2+1)-dimensional modified dispersive water wave equation. *Comput. Math. Appl.* **77**, 2086–2095 (2019)

- Saeedi, M., Moradi, M., Hosseini, M., Emamifar, A., Ghadimi, N.: Robust optimization based optimal chiller loading under cooling demand uncertainty. *Appl. Therm. Eng.* **148**, 1081–1091 (2019)
- Seadawy, A.R., Arshad, M., Lu, D.: The weakly nonlinear wave propagation theory for the Kelvin–Helmholtz instability in magneto hydrodynamics flows. *Chaos Solitons Fract.* **139**, 110141 (2020)
- Shehzad, K., Seadawy, A.R., Wang, J., Arshad, M.: Multi peak solitons and breather types wave solutions of unstable NLSes with stability and applications in optics. *Opt. Quant. Elec.* **55**, 7 (2023)
- Singh, S., Kaur, L., Sakthivel, R., Murugesan, K.: Computing solitary wave solutions of coupled nonlinear Hirota and Helmholtz equations. *Physica A: Stat. Mech. Appl.* **560**, 125114 (2020)
- Song, J.H., Maier, M., Luskin, M.: Nonlinear eigenvalue problems for coupled Helmholtz equations modeling gradient-index graphene waveguides. *J. Comput. Phys.* **423**, 109871 (2020)
- Sun, W., Wang, H., Qu, R.: A novel data generation and quantitative characterization method of motor static eccentricity with adversarial network. *IEEE Trans. Power Electr.* **38**(7), 8027–8032 (2023)
- Tamilselvan, K., Kanna, T., Khare, A.: Nonparaxial elliptic waves and solitary waves in coupled nonlinear Helmholtz equations. *Commun. Nonlinear Sci. Num. Simul.* **39**, 134–148 (2016)
- Wang, L., She, A., Xie, Y.: The dynamics analysis of Gompertz virus disease model under impulsive control. *Sci. Rep.* **13**(1), 10180 (2023)
- Wazwaz, A.M.: *Partial Differential Equations and Solitary Waves Theory*. Springer, Heidelberg (2009)
- Wen, X.Y., Xu, X.G.: Multiple soliton solutions and fusion interaction phenomena for the (2+1)-dimensional modified dispersive water-wave system. *Appl. Math. Comput.* **219**, 7730–7740 (2013)
- Xiang, J., Liao, J., Zhu, Z., Li, P., Chen, Z., Huang, J., Chen, X.: Directional fluid spreading on microfluidic chip structured with microwedge array. *Phys. Fluids* **35**(6), 62005 (2023)
- Xiao, Y., Zhang, Y., Kaku, I., Kang, R., Pan, X.: Electric vehicle routing problem: a systematic review and a new comprehensive model with nonlinear energy recharging and consumption. *Renew. Sustain. Energy Rev.* **151**, 111567 (2021)
- Xu, S., Dai, H., Feng, L., Chen, H., Chai, Y., Zheng, W.X.: Fault estimation for switched interconnected nonlinear systems with external disturbances via variable weighted iterative learning. *IEEE Trans. Circuits Syst. II: Exp. Briefs* (2023) <https://doi.org/10.1109/TCSII.2023.3234609>
- Yu, D., Zhang, T., He, G., Nojavan, S., Jermisittiparsert, K., Ghadimi, N.: Energy management of wind-PV-storage-grid based large electricity consumer using robust optimization technique. *J. Energy Storage* **27**, 101054 (2020)
- Yuan, Z., Wang, W., Wang, H., Ghadimi, N.: Probabilistic decomposition-based security constrained transmission expansion planning incorporating distributed series reactor. *IET Gen. Trans. Distrib.* **14**(17), 3478–3487 (2020)
- Zahedi, R., Golivari, S.: Investigating threats to power plants using a carver matrix and providing generalized soliton s: a case study of Iran. *Int. J. Sustain. Energy Environ. Res.* **11**(1), 23–36 (2022)
- Zhang, J., Khayatnezhad, M., Ghadimi, N.: Optimal model evaluation of the proton exchange membrane fuel cells based on deep learning and modified African vulture optimization algorithm. *Energy Sources A* **44**, 287–305 (2022)
- Zhong, Q., Han, S., Shi, K., Zhong, S., Kwon, O.: Co-Design of adaptive memory event-triggered mechanism and aperiodic intermittent controller for nonlinear networked control systems. *IEEE Trans. Circuit Syst. II Exp. Briefs* **69**(12), 4979–4983 (2022)
- Zhou, X., Ilhan, O.A., Manafian, J., Singh, G., Tuguz, N.S.: N-lump and interaction solutions of localized waves to the (2+1)-dimensional generalized KDKK equation. *J. Geo. Phys.* **168**, 104312 (2021)

Publisher's Note Springer Nature remains neutral with regard to jurisdictional claims in published maps and institutional affiliations.

Springer Nature or its licensor (e.g. a society or other partner) holds exclusive rights to this article under a publishing agreement with the author(s) or other rightsholder(s); author self-archiving of the accepted manuscript version of this article is solely governed by the terms of such publishing agreement and applicable law.

Authors and Affiliations

Yufeng Qian¹ · Jalil Manafian^{2,3} · Mohammed Asiri⁴ · Khaled Hussein Mahmoud⁵ · Ali Ihsan Alanssari⁶ · Abdullah Saad Alsubaie⁵

✉ Jalil Manafian
j_manafianheris@tabrizu.ac.ir

Yufeng Qian
yfqian@aliyun.com

Mohammed Asiri
mrasiri@kku.edu.sa

Khaled Hussein Mahmoud
k.hussein@tu.edu.sa

Ali Ihsan Alanssari
ali.ih.eng@nuc.edu.iq

Abdullah Saad Alsubaie
asubaie@tu.edu.sa

¹ School of Science, Hubei University of Technology, Wuhan 430068, China

² Department of Applied Mathematics, Faculty of Mathematical Sciences, University of Tabriz, Tabriz, Iran

³ Natural Sciences Faculty, Lankaran State University, 50, H. Aslanov str., Lankaran, Azerbaijan

⁴ Department of Clinical Laboratory Sciences, College of Applied Medical Sciences, King Khalid University, Abha, Saudi Arabia

⁵ Department of Physics, College of Khurma University College, Taif University, P.O. Box 11099, Taif 21944, Saudi Arabia

⁶ Al-Nisour University College, Baghdad, Iraq